



MOLECULAR LEVEL COMPOSITE OF PBT/ABPBI:
PHASE RELATIONSHIPS, PROCESSING AND PROPERTIES

T. Helminiak
W. -F. Hwang
D. Wiff
C. Benner
G. Price

Polymer Branch
Nonmetallic Materials Division

October 1982

Final Report for Period January 1980 to August 1981

Approved for public release; distribution unlimited.

20040223062

MATERIALS LABORATORY
AIR FORCE WRIGHT AERONAUTICAL LABORATORIES
AIR FORCE SYSTEMS COMMAND
WRIGHT-PATTERSON AIR FORCE BASE, OHIO 45433

BEST AVAILABLE COPY

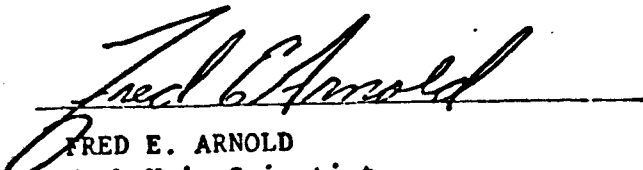
OFFICIAL FILE COPY

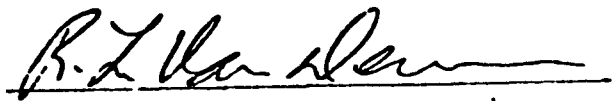
NOTICE

When Government drawings, specifications, or other data are used for any purpose other than in connection with a definitely related Government procurement operation, the United States Government thereby incurs no responsibility nor any obligation whatsoever; and the fact that the government may have formulated, furnished, or in any way supplied the said drawings, specifications, or other data, is not to be regarded by implication or otherwise as in any manner licensing the holder or any other person or corporation, or conveying any rights or permission to manufacture use, or sell any patented invention that may in any way be related thereto.

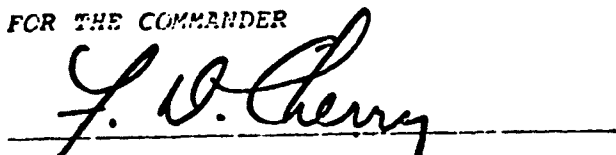
This report has been reviewed by the Office of Public Affairs (ASD/PA) and is releasable to the National Technical Information Service (NTIS). At NTIS, it will be available to the general public, including foreign nations.

This technical report has been reviewed and is approved for publication.


FRED E. ARNOLD
Work Unit Scientist


R. L. VAN DEUSEN, CHIEF
Polymer Branch
Nonmetallic Materials Division

FOR THE COMMANDER


F. D. CHERRY, Acting Chief
Nonmetallic Materials Division

"If your address has changed, if you wish to be removed from our mailing list, or if the addressee is no longer employed by your organization please notify AFWAL/MLBP, W-PAFB, OH 45433 to help us maintain a current mailing list".

Copies of this report should not be returned unless return is required by security considerations, contractual obligations, or notice on a specific document.

UNCLASSIFIED

SECURITY CLASSIFICATION OF THIS PAGE (When Data Entered)

REPORT DOCUMENTATION PAGE		READ INSTRUCTIONS BEFORE COMPLETING FORM
1. REPORT NUMBER AFWAL-TR-82-4039	2. GOVT ACCESSION NO.	3. RECIPIENT'S CATALOG NUMBER
4. TITLE (and Subtitle) MOLECULAR LEVEL COMPOSITE OF PBT/ABPBI: PHASE RELATIONSHIPS, PROCESSING AND PROPERTIES		5. TYPE OF REPORT & PERIOD COVERED Technical Report Final January 1980-August 1981
		6. PERFORMING ORG. REPORT NUMBER
7. AUTHOR(s) W.-F. Hwang, D.R. Wiff, C.B. Benner and G. Price, Univ. Dayton Research Institute, Polymer Science, T.E. Helminiak, Wright Aero. Mat. Lab.		8. CONTRACT OR GRANT NUMBER(s)
9. PERFORMING ORGANIZATION NAME AND ADDRESS Materials Laboratory (AFWAL/MLBP) AF Wright Aeronautical Laboratories, AFSC Wright-Patterson Air Force Base, OH 45433		10. PROGRAM ELEMENT, PROJECT, TASK AREA & WORK UNIT NUMBERS 61102F 2303Q307
11. CONTROLLING OFFICE NAME AND ADDRESS Materials Laboratory (AFWAL/MLBP) AF Wright Aeronautical Laboratories, AFSC Wright-Patterson Air Force Base, OH 45433		12. REPORT DATE October 1982
		13. NUMBER OF PAGES 57
14. MONITORING AGENCY NAME & ADDRESS (if different from Controlling Office)		15. SECURITY CLASS. (of this report) Unclassified
15a. DECLASSIFICATION/DOWNGRADING SCHEDULE		
16. DISTRIBUTION STATEMENT (of this Report) Approved for public release, distribution unlimited.		
17. DISTRIBUTION STATEMENT (of the abstract entered in Block 20, if different from Report)		
18. SUPPLEMENTARY NOTES		
19. KEY WORDS (Continue on reverse side if necessary and identify by block number)		
Molecular Composites	Rod-like Polymer	Phase Diagrams Blends
Halpin-Tsai Equation	Heterocyclic Polymer	SALS Critical Concen.
Rule of Mixtures	Ternary Systems	SAXS Nematic Phase
Mechanics of Composites		Polyblends
20. ABSTRACT (Continue on reverse side if necessary and identify by block number)		
<p>The concentrated solution phase relationships and bulk polymer morphology of a solvent/rigid rod/flexible coil system were investigated. The solvent was a mixture of two strong acids. The rigid rod polymer was poly-para-phenylene-benzobisthiazole (PBT). The flexible coil polymer was poly-2,5(6) benzimidazole (ABPBI). The concentrated solution and bulk polymer morphologies were investigated by means of polarized optical microscopy, small angle light scattering, scanning electron microscopy, and wide angle x-ray diffraction techniques.</p>		

UNCLASSIFIED

SECURITY CLASSIFICATION OF THIS PAGE(When Data Entered)

Above a critical concentration, C_{Cr} , the pseudo ternary solution separated into two coexisting phases, one optically anisotropic (liquid crystalline) and the other isotropic. The anisotropic domains were highly birefringent. They contained primarily the PBT macromolecules oriented preferentially along a domain axis. Numerical results of C_{Cr} , determined experimentally, were in good agreement with calculated predictions. Aggregates composed of PBT molecules were observed to be dispersed in a continuous matrix for vacuum cast films. These results strongly indicate the dominance of entropic effects in the thermodynamics of rigid rod-like polymer flexible coil-like polymer mixtures. The feasibility of processing these novel mixtures into "molecular level composites" (molecular composite) having rigid rod PBT macromolecules dispersed in a continuous ABPBI matrix, as inferred from phase relationship results is demonstrated and validated. These composites not only possess excellent tensile properties, but they also may be "tuned" to a desired combination of properties e.g.; uniaxial modulus, ultimate tensile strength, and elongation.

UNCLASSIFIED

SECURITY CLASSIFICATION OF THIS PAGE(When Data Entered)

FOREWORD

This report was prepared by the Polymer Branch, Nonmetallic Materials Division. The work was initiated under Project No. 2303, "Research to Define the Structure Property Relationships," Task No. 2303Q3, Work Unit Directive 2303Q307, "Structural Resins." It was administered under the direction of the Materials Laboratory, Air Force Wright Aeronautical Laboratories, Air Force Systems Command, Wright-Patterson Air Force Base, Ohio, with Dr. F. E. Arnold as the AFWAL/ML Work Unit Scientist. Co-authors were Dr. T. Helminiak, Materials Laboratory (AFWAL/MLBP); and Dr. Wen-Fang Hwang, Dr. D. Wiff, and Mr. C. Benner, University of Dayton Research Institute.

This report covers research conducted from January 1980 to August 1981.

TABLE OF CONTENTS

SECTION		PAGE
I	INTRODUCTION	1
II	EXPERIMENTAL	5
	1. Materials	5
	2. Methods and Sample Preparations	5
	3. Instruments	7
III	RESULTS AND DISCUSSION	8
	1. Conformation Characteristics and Flexibility of the ABPBI Chain	8
	2. Phase Relationship of Solvent/PBT/ABPBI Ternary Systems	15
	3. Molecular Composite of PBT/ABPBI	33
IV	CONCLUSIONS	46
	REFERENCES	47

LIST OF ILLUSTRATIONS

FIGURE		PAGE
1a	Spherulites of 4.75 wt% Moisture Contaminated ABPBI Solution in 97.5 MSA/2.5 CSA, Crossed Nicol.	9
1b	Radiating Fibrous Structure of ABPBI Spherulites.	11
2	Third Order Total Energies of 2,5 Bi-Benzimidazole as a Function of the Torsional Angles, ψ , Between Benzimidazole Planes.	12
3	Schematic Representation of ABPBI Chain of Fully Extended Configuration by a Virtual Bond Model, and its Geometric Parameters.	14
4a	OM of a Biphaseic Solution of 4.475 wt% 20/80 PBT (IV=18)/ABPBI in 97 MSA/2.5 CSA, Showing "Islands" of Colored Liquid Crystalline Domains Dispersed in an Isotropic Background. Crossed Nicol.	16
4b	OM of a Biphaseic Solution (same as in (a)) Under the Influence of External Shear, Where LC Domains Are Elongated in the Shearing Direction. Crossed Nicol.	16
4c	OM of a Biphaseic Solution of 4.35 wt% 20/80 PBT (IV=18)/ABPBI in 97.5 MSA/2.5 CSA. Size of LC domains is smaller than that in (a).	19
5	OM of the Mostly Anisotropic Region of an 60/40 PBT (IV=18)/ABPBI Hand-Sheared Quenched Film (HS F) from Solution with $C > C_{cr}$, Showing Distinct Rod-Like Superstructures. Crossed Nicol.	20
6	SALS H_V Pattern of the Optically Anisotropic Region in a 60/40 PBT (IV=18)/ABPBI HSQF. Sample to film distance = 12.5 cm.	21
7	Calculated Ternary Phase Diagram with Experimental Data Points for Solvent/PBT (IV=18, $X_2 = 300$)/ABPBI ($X_3 = 300$) System.	23
8	Temperature-Concentration Phase Diagrams for 60/40 and 40/60 PBT (IV=18)/ABPBI Solutions.	24
9	SEI (Secondary Electron Image) of the Liquid Nitrogen Freeze Fracture Surface of a 20/80 PBT (IV=18)/ABPBI Vacuum Cast Film.	27

LIST OF ILLUSTRATIONS (Cont'd)

FIGURE		PAGE
10a	SEI of the Film Surface of a 20/80 PBT (IV=18)/ABPBI Vacuum Cast Film.	28
10b	BSEI (Back-Scattering Electron Image) of (a).	29
11a	SEI of the Film Surface of a 60/40 PBT (IV=18)/ABPBI Vacuum Cast Film.	30
11b	BSEI of (a). Size of Aggregates is much Larger than that shown in Figure 10.	31
12	Uniaxial Modulus, E_{11} of 30/70 PBT (IV=31)/ABPBI NHT1010 Composite as a Function of Aspect Ratio, ζ . $E_f = 44$ MSI, $E_m = 5.2$ MSI.	36
13	SEI of a Tensile Broken 30/70 PBT (IV=31)/ABPBI NHT1010 Composite Fiber.	38
14a	SEI of the Internal Surface of a Peeled 30/70 PBT (IV=31)/ABPBI NHT1010 Composite Fiber.	39
14b	BSEI of (a).	40
15	WAXD of ABPBI NHT1010 Fiber 8 Filaments. Norelco 40kv 20 MA. 168 hrs exposure.	41
16a	WAXD of As-Spun 30/70 PBT (IV=31)/ABPBI Composite Fiber, 8 Filaments. Norelco 40kv 20MA, 168 hrs exposure.	43
16b	WAXD of 30/70 PBT (IV=31)/ABPBI NHT1010 Composite Fiber. 8 Filaments, Norelco 40kv 20MA, 168 hrs exposure.	44

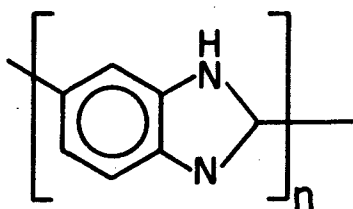
LIST OF TABLES

TABLE		PAGE
1	Comparison of Parameters Characterizing Chain Rigidity	15
2	Critical Concentrations, C_{cr} , of ABPBI/PBT Blends in 97.5 MSA/2.5/2.5 CSA at Room Temperature 22-250C	22
3	Phase Compositions and Solution Characteristics of a 60/40 PBT (IV=18)/ABPBI Blend in 97.5 MSA/2.5 CSA as a Function of Polymer Concentrations	26
4	Description and Tensile Properties of 30/70 PBT (IV=31)/ABPBI Blend and ABPBI Fibers	35

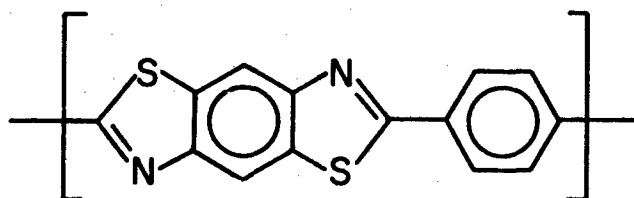
SECTION I

INTRODUCTION

This report contains the continuing efforts to investigate the concept of using a rigid rod-like wholly aromatic heterocyclic polymer (poly-para-phenylene benzbisthiazole, PBT) to reinforce a flexible coil-like aromatic heterocyclic polymer (poly-2,5(6) benzimidazole, ABPBI). The intent (Reference 1) is to form a PBT/ABPBI composite on the molecular level, analogous to advanced chopped fiber composites on the macroscopic level with similar or superior properties.



AB-PBI



PBT

Previously attempts (References 2,3) were made to obtain molecular level composite films via casting and precipitation of dilute solutions (1.5 wt% polymers concentration) of various PBT/ABPBI compositions in methane sulfonic acid (MSA). Post-film treatments such as mechanical stretching and solvent stretching demonstrated that the mechanical properties as well as the film morphology could be significantly altered.

One of the most important parameters in controlling the uniaxial modulus and ultimate tensile strength in the fiber composite technology is the length (l) to diameter (d) ratio, aspect ratio (ζ), of the reinforcing fiber. Increasing this aspect ratio either by increasing the length or decreasing the diameter of the fiber can increase the modulus of the composite up to two orders of magnitude (Reference 4). Following this reasoning, the ultimate reinforcing fiber would be a single extended rigid rod-like polymer molecule. This is the basic idea in our efforts to obtain a molecular composite by dispersing rigid rod-like molecules in a continuous matrix. A stretched or oriented PBT/ABPBI molecular composite system can be viewed as being transversely

isotropic, i.e., a system of uniaxially aligned PBT molecules randomly positioned in an ABPBI matrix. It has symmetry properties in the plane normal to that of the aligned direction. For such a system, employment of the semiempirical Halpin - Tsai relationship (Reference 4) enables one to predict the uniaxial modulus of the composite, E_{11} , and its dependence on the aspect ratio, $\zeta = 2(l/d)$, from material properties of constituents. This relationship is given by

$$E_{11}/E_m = (1 + \zeta \eta v_f)/(1 - \eta v_f), \quad (1)$$

where

$$\eta = (E_f/E_m - 1) (E_f/E_m + \zeta)^{-1}, \quad (2)$$

v_i is the volume fraction, E_i the modulus of the constituents, and subscripts f and m refer to fiber and matrix, respectively. As the aspect ratio becomes large, E_{11} approaches the limiting upper bound:

$$E_{11} \approx E_f v_f + E_m v_m \quad (3)$$

Thus, if one could obtain a molecular composite of nearly perfectly aligned PBT molecules dispersed in an ABPBI matrix, the above rule of mixtures should hold, where E_f represents the ultimate modulus of PBT molecules, and E_m the modulus of matrix polymer at that particular state of orientation when fabricated.

One drawback in the fabrication process is that these high temperature polymers, ABPBI and PBT, are highly intractable and are not amenable to melt processing.* However, these polymer blends can be processed from a common solvent. Thus, the solution behavior, especially the phase relationship of this ternary system, becomes one of the controlling factors in the actual processing.

*These systems do not show T_m or T_g , therefore, do not amend themselves to standard polymer characterization.

In a recent theory by Flory (Reference 5), the statistical thermodynamics of a ternary isodiametrical solvent, a rigid rod-like polymer and a flexible coil-like polymer system was considered. The theoretical treatment was restricted to "athermal" mixtures, i.e., systems in which interactions between polymers and solvent molecules were ignored. In the present study, this theory was applied as a guide for determining, at thermodynamic equilibrium, the upper critical concentration (isotropic to biphasic transition) above which regions or domains of solely rigid rod molecules would exist. Liquid crystalline domains have the molecules aligned relative to the axis of the domain. The orientation of the molecules within a domain was characterized by a "disorientation factor, γ " (Reference 6), (see Figure 1, in Reference 6 for definition). This equilibrium phase segregation behavior was attributed to the profound disparity of the geometry and rigidity of the two polymer components. Experimental evidences for such a ternary solution behavior have been rare. One recent study (Reference 7) demonstrated a general agreement with the theory (Reference 5).

The premise of the present investigation was that an understanding of the concentrated solution behavior prior to processing would enable one to control the solution morphology, and thus the processing and properties of the bulk composite. The present investigation considers, for the first time, the correlation between phase relationship, morphology, and processing of a pseudo* ternary solution-solvent/PBT/ABPBI and properties of molecular composites prepared from these solutions.

In the first part of this report, the conformation characteristics and flexibility of the ABPBI chain are discussed in order to establish the validity of the assumed, solvent/rigid rod-like/flexible coil-like, ternary systems. Conformation analysis of a model compound of ABPBI, 2,5' bi-benzimidazole, was carried out by the PCILO method (Reference 8).

*Mixed 97.5 vol% methane sulfonic acid (MSA) with 2.5 vol% chlorosulfonic acid (CSA) was treated as a single solvent compound in the theoretical calculations.

Moments of the end-to-end vector of ABPBI chains which reflect how persistent or flexible these chains are in the direction of the benzimidazole ring axis (x direction), were calculated using a virtual bond model (Reference 9). Secondly, phase relationship of this ternary system as a function of concentration, temperature, and molecular weight of the rigid rod-like PBT polymer is presented. Quantitative comparison with theory (Reference 5) is made. The optimum conditions for processing as inferred from the phase relationship study are demonstrated, and finally, characterization and tensile properties of bulk specimens are presented.

Preliminary results of this report were presented at ACS National Meeting, Atlanta, Georgia, in March 1981.

SECTION II

EXPERIMENTAL

1. MATERIALS

Poly-2,5(6) benzimidazole (ABPBI) was synthesized by Whittaker Corporation (Reference 10). The average inherent viscosity measured in sulfuric acid was 14 dl/g. The average molecular weight measured by an end-capping experiment (Reference 10) was about 100,000 g/mole. Poly-para-phenylenebenzobisthiazole (PBT) was synthesized by Dr. James Wolfe of Stanford Research International. Two PBT polymers with inherent viscosities of 18, and 31 dl/g (measured in dilute methanesulfonic acid solution) were used in this investigation. The weight-averaged molecular weights of the two PBT polymers were estimated to be 30,300, and 41,000 g/mole, respectively, using the relationships (Reference 11).

$$\{\eta\} = 4.86 \times 10^{20} \frac{d_H^{0.2}}{M_L} \left(\frac{M_\eta}{M_L} \right)^{1.8}$$

$$M_\eta^{1.8} = M_w^{1.8} \left(\frac{1}{n+1} \right)^{1.8} \frac{\Gamma(1.8+h+1)}{\Gamma(h+1)}$$

derived for polymer chains in the rodlike limit. Here the numerical values for d_H , the hydrodynamic diameter of a chain element, and M_L the mass per unit length were taken as 7 \AA and 22 \AA^{-1} throughout the calculation (Reference 11). The heterogeneity factor, $h=(M_w/M_\eta) - 1$, was assumed to be 2. $\Gamma(x)$ is the Gamma function.

Except for vacuum drying prior to solution preparation, both ABPBI and PBT were used as received without further purification. The solvent used was a mixed solvent consisting of 97.5 vol% methanesulfonic acid (MSA) and 2.5 vol% chlorosulfonic acid (CSA). Both were redistilled. The CSA was added primarily to scavenge water.

2. METHODS AND SAMPLE PREPARATIONS

Ternary solutions were prepared by mixing predetermined weight compositions of PBT/ABPBI in the solvent system on a magnetic stirrer at room temperature (22-25°C) until all the polymer was dissolved. This

usually took about a week, depending upon the concentration of polymers. The concentration of these solutions was expressed in the unit of weight percentage.

The critical concentration was defined as the maximum concentration of polymers in a solution at which it was still optically isotropic. This was determined by slowly titrating an originally biphasic, stir opalescent solution of known concentration with solvent until a point was reached at which the solution became isotropic and stir-opalescence ceased. Due to the high viscosity of the solution, the solution was stirred for at least three days between titrations to ensure a complete dissolution.

The biphasic (nematic and isotropic phases) to isotropic transition temperature, T_{N-I} , of the solution was determined by the following procedure. A drop of the concentrated solution was pressed between a microscope slide and a thin cover glass. It was heated on a hot stage at a heating rate of 20C/min. The solution was observed between crossed polars until a temperature was reached at which liquid crystalline domains disappeared and the viewing area of the microscope resembled that observed for an isotropic solution.

Optical microscopy examination of the phase separation behavior was carried out by sealing a thin layer of the solution between a glass slide and a cover glass sealed with paraffin wax to prevent moisture contamination.

Bulk composite specimens for morphology characterization and mechanical testing were prepared in film and fiber forms. The film was prepared by handshearing a drop of solution at or below its critical concentration point between glass plates, and subsequently quenched in deionized water where it remained over night to allow complete leaching of the acid. These film specimens were denoted as hand-sheared quenched films (HSQF). Before the solution completely solidified, some of the specimens were elongated to a desired length. Composite fibers were made by extruding solution through a single-hole 254 μ spinnerette into a quenching bath of deionized water at room temperature. The partially

coagulated solution was subsequently drawn between two rollers on a fiber drawing machine and wound on a collecting roll immersed in a water bath. The entire roll with fiber remained in water for 24 hours. The initial draw ratio was 3.4. Some of the films and fibers were then neutralized in NH_4OH overnight to leach out all the residual acids. The neutralized samples were further washed with running deionized water. The bulk specimens were then air dried at ambient conditions. Heat treatments of composite fibers were carried out by passing them through an oven in air atmosphere while under a constant strain on the fiber drawing machine. The residence time of fiber in the oven was 30 sec. Pure ABPBI fibers were spun and heat treated in the similar manner as the composite fibers. Single filaments were centerline mounted on special one inch gauge length paper tabs with epoxy glue. Tensile testings were carried out at a constant strain rate of 0.02 min.^{-1} . The fiber diameter was determined by an optical microscope.

3. INSTRUMENTS

Morphology characterizations were performed by standard optical microscopy, small-angle light (laser) scattering, scanning electron microscopy, and wide-angle-x-ray diffraction techniques. Instruments used were a Bausch & Lomb LI-2 polarizing light microscope, Mettler FP 52 hot stage with -20 to 300°C temperature range, Spectra-physics 155 He-Ne laser, ETEC Autoscan SEM with backscatter detector, and Elliot GX 20 rotating anode x-ray generator. Tensile testings were carried out on an Instron 1102 tensile tester.

SECTION III

RESULTS AND DISCUSSION

1. CONFORMATION CHARACTERISTICS AND FLEXIBILITY OF THE ABPBI CHAIN

Before examining the phase relationships of this ternary system, it was imperative to examine the conformation characteristics of ABPBI and PBT molecules in solution to elucidate the origin for the formation of optically anisotropic liquid crystalline (LC) phases in these systems.

The PBT molecules when dissolved in MSA or 97.5% MSA/2.4% CSA have been shown to exhibit an extended rigid rod-like conformation (Reference 12). As expected, PBT solutions were optically anisotropic at $C > C_{cr}$ and they formed stable nematic LC solution indicative of a high degree of order (Reference 12).

The solution behavior of ABPBI was first examined by Delano (Reference 10) and coauthors. They showed, with exceptions in the formic acid and in a mixed formic acid/m-cresol solvent, that ABPBI did not form a liquid crystalline solution from any other solvent investigated including concentrated sulfuric acid. The observed LC behavior (occurred at 2 wt% ABPBI concentration) may be understood as arising from the protonation of the imidazole ring of the polymer in the strong protonating solvent such as formic acid (FA). A considerable number of unsaturated nitrogen atoms on these rings react with FA molecules to produce a polyelectrolyte in solution as was observed for FA solutions of poly (2,2'-4,4'-oxydiphenylene)-5,5'-bi'benzimidazole) (PBI) (Reference 13). A considerable uncoiling of the polymer chains may occur due to the presence of the charges along them so that they behave more as rod-like chains (References 13,14,15). This may be the case for ABPBI in FA solution. Similarly, when a drop of an originally isotropic ABPBI solution (4.75 wt% concentration in 97.5 MSA/2.5 CSA), sandwiched between a glass slide and a thin cover glass, was exposed to the moisture in the air at ambient room conditions the solution became greyish opaque. Spherulites having diameters of 50-200 microns were observed as shown in Figure 1a, the sign of birefringence of these spherulites was determined to be negative by the first order red-plate method. At

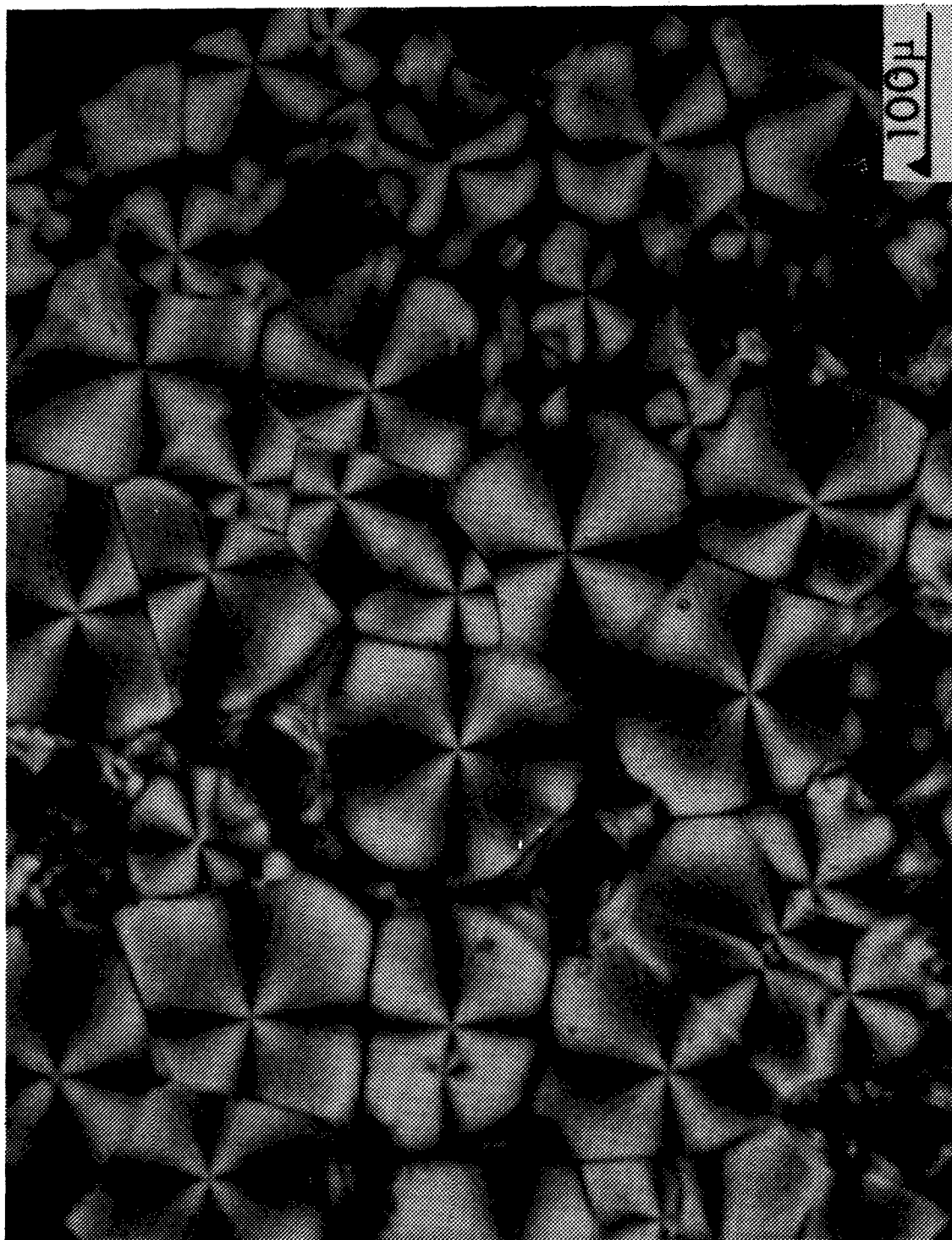
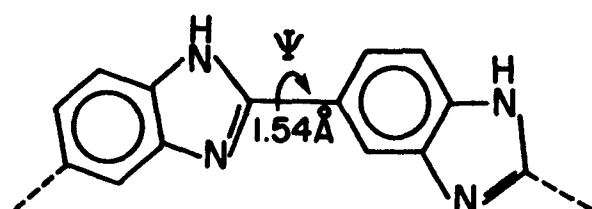


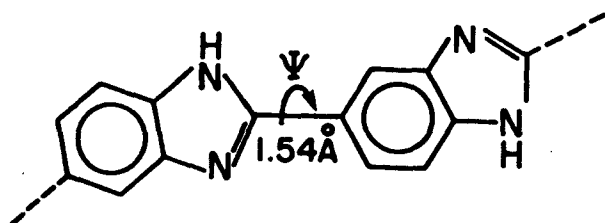
Figure 1a. Spherulites of 4.75 wt% Moisture Contaminated ABPI Solution in 97.5 MSA/2.5 CSA, Crossed Nicol.

larger magnification (Figure 1b), a radiating fibrous structure can be clearly seen. This may be interpreted that the water molecules caused a drastic increase in the ionic strength of MSA which in turn caused the protonation of ABPBI chains, similar to that occurring in FA solution. The uncoiled polyionic chain complex has a helical rod-like conformation which aggregates to form a spherulite with the helical axis oriented radially. Detailed analysis of the orientation of the ABPBI crystallites inside a spherulite by electron diffraction and microscopy techniques is currently underway. This along with the complete ABPBI spherulite study will be the subject of a later report.

PCILO conformational calculations have been made on a model compound of ABPBI, 2,5' bi-benzimidazole. The input geometry, bond length and bond angles, was taken from the reported (Reference 16) x-ray crystal structure of benzimidazole. The C2-C5' bond length between benzimidazole rings was taken as 1.54 Å. Rotation around this bond shows the two extreme planar conformations of 2,5'-bi-benzimidazole. Throughout the calculation no geometry optimization was carried out. The result is shown in Figure 2. The same results were obtained for a



cis-form
2,5 Bi-benzimidazole



trans-form
2,5 Bi-benzimidazole

trimer of benzimidazole. In essence, the result indicates that monomer units along the ABPBI chain is essentially oscillating in a rather broad ($\pm 90^\circ$ with respect to the transconformation) potential well of 3.5 kcal/mole in depth. It was pointed (References 9,17) out that for long

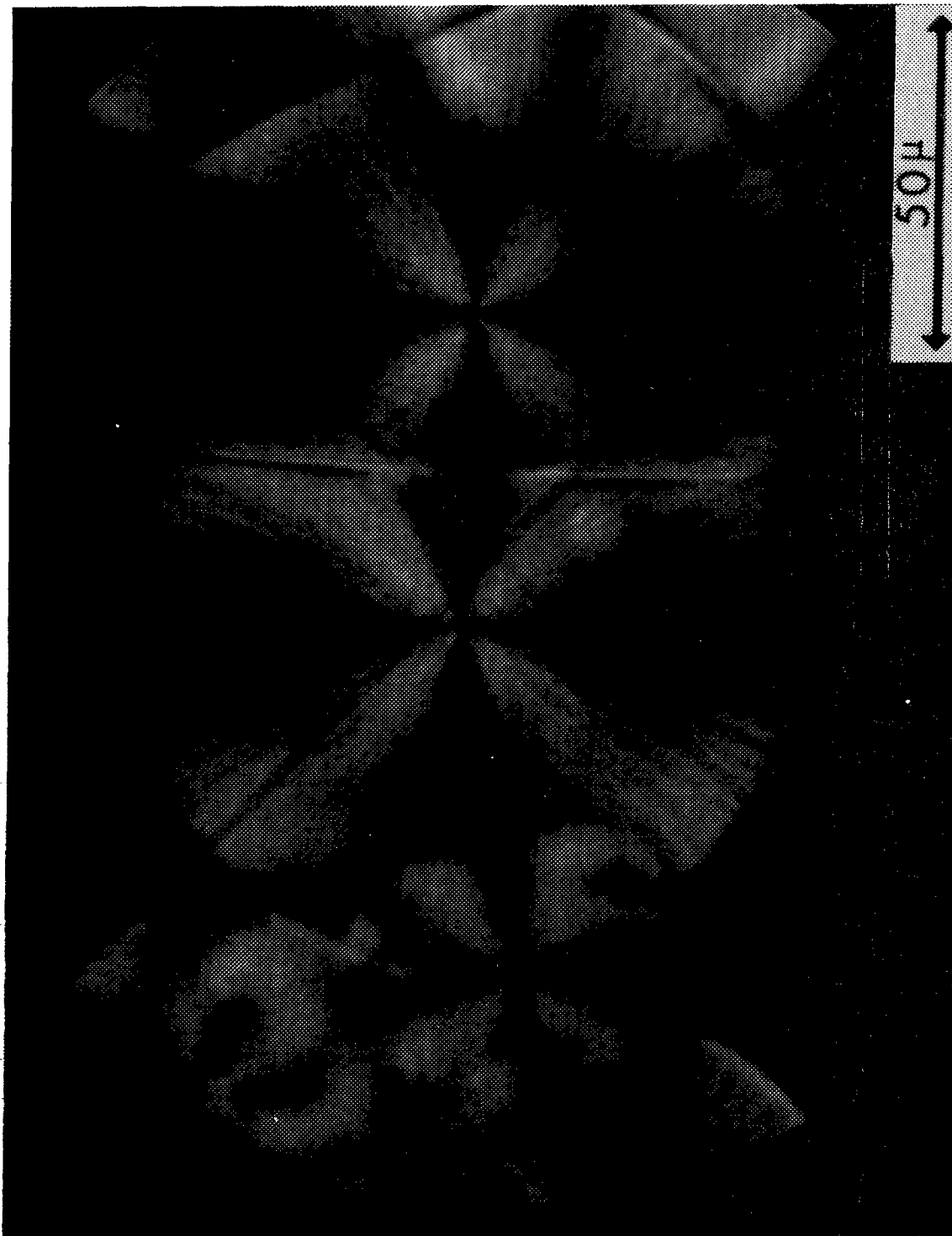


Figure 1b. Radiating Fibrous Structure of ABPI Spherulites.

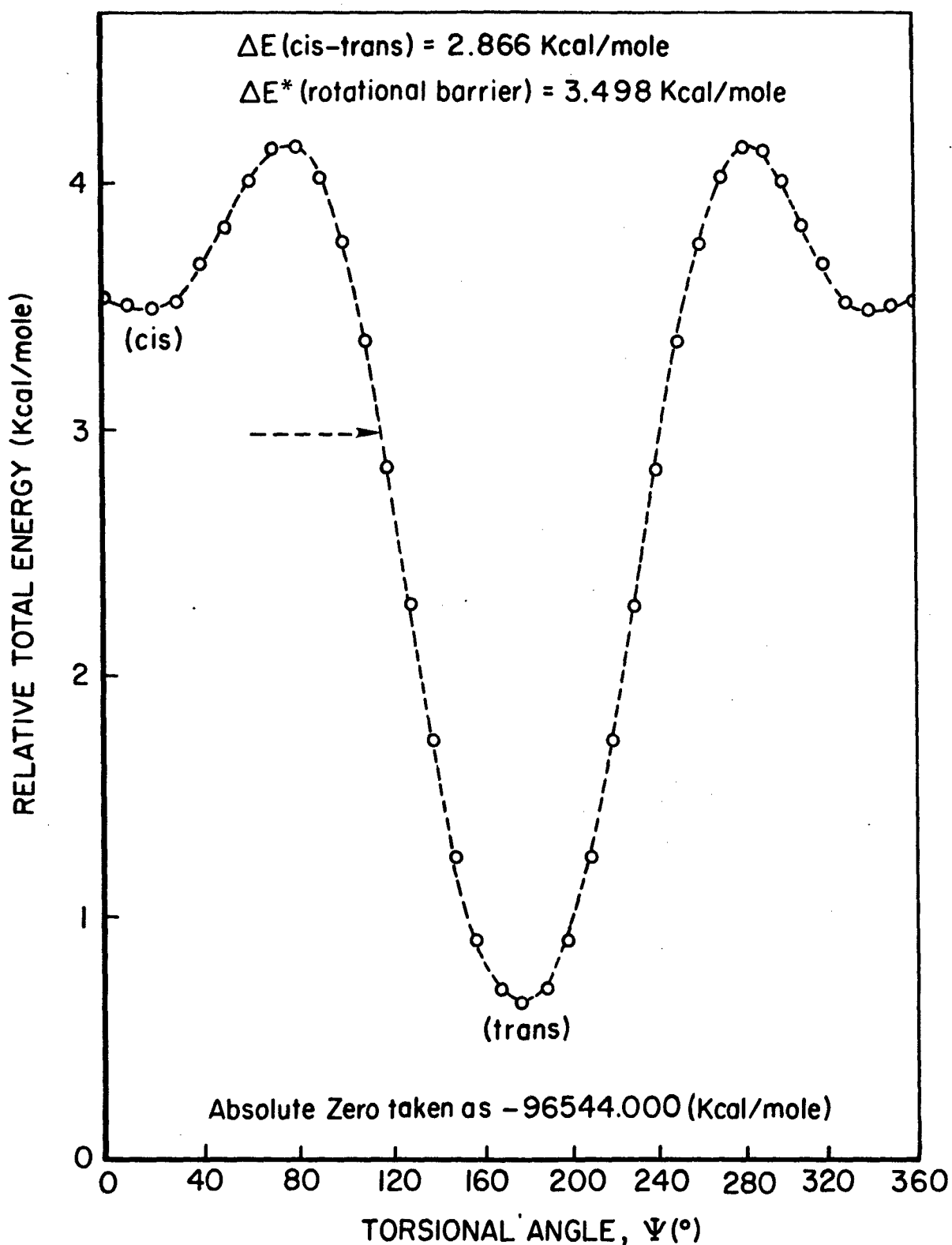


Figure 2. Third Order Total Energies of 2,5 Bi-Benzimidazole as a Function of the Torsional Angles, ψ , Between Benzimidazole Planes.

polymer chains these torsional oscillations are sufficient to make the chain coil. Furthermore, due to the localized nature of orbitals in the PCILO method which sacrifice the delocalization energy term, the PCILO method tends to overestimate the rotational barrier height. In view of this, we will assume free rotation between benzimidazole planes for the following calculation.

The first and second moments of the end-to-end vector \vec{r} , of ABPBI chain is considered. These moments are signified as indexes of the character of the distribution $W(\vec{r})$ of \vec{r} , which are direct measures of the polymer chain flexibility. They were calculated following the statistical scheme and convention of Flory (Reference 18), and using the geometrical parameters presented by a virtual bond model (Reference 9). The geometrical parameters and the virtual bond model of the ABPBI chain is schematically represented in Figure 3. These geometry parameters, $\ell_i \delta_i$, and ζ_i (for their definitions see Figure 3) were determined from the reported (Reference 16) molecular geometry of benzimidazole, and were held fixed. The configuration of the ABPBI chain shown in Figure 3, in which the virtual bonds are in planar zigzag array, is the one of maximum extension. As shown in Figure 2, the torsional potentials affecting ψ_i are symmetric with respect to the planar conformations at $\psi_i = 0$ and π . Hence, $\langle \sin \psi_i \rangle$ is zero. In the limit of infinite chain lengths, the persistence length (first moment of \vec{r}) and the characteristic ratio (second moment of \vec{r}) along the extended chain direction (\hat{X}) of a polymer chain were shown to be (Reference 9)

$$\langle x_{\infty} \rangle / \ell = \frac{u + \beta v}{1 - \alpha} \quad (4)$$

$$C_{\infty} = b / \ell = \{ (1 + \alpha) / (1 - \alpha) \}^{1/2} (u + v)^2 \quad (5)$$

where $\alpha = \cos \delta$, $\beta = \sin \delta$, $u = \cos \zeta$, $v = \sin \zeta$, and b the length of Kuhn segment. For ABPBI, $\alpha = 0.866$, $\beta = 0.5$, $\mu = 0.954$, $v = 0.200$. The calculated $\langle x_{\infty} \rangle / \ell$, $\langle x_{\infty}^2 \rangle$, b / ℓ and b values along with those calculated for polyamides, polyesters, and polyethylenes are summarized in Table 1. In contrast to the mesogenic polyamides and polyesters, an

GEOMETRICAL
PARAMETERS

$\ell = 5.9027 \text{ \AA} = \text{VIRTUAL BOND LENGTH}$
 $\delta = 30^\circ = \text{ANGLE BETWEEN DIRECTION OF CONSECUTIVE RING AXIS}$
 $\xi = 17.4^\circ = \text{ANGLE BETWEEN VIRTUAL BOND AND RING AXIS}$

DASHED LINE = VIRTUAL BOND

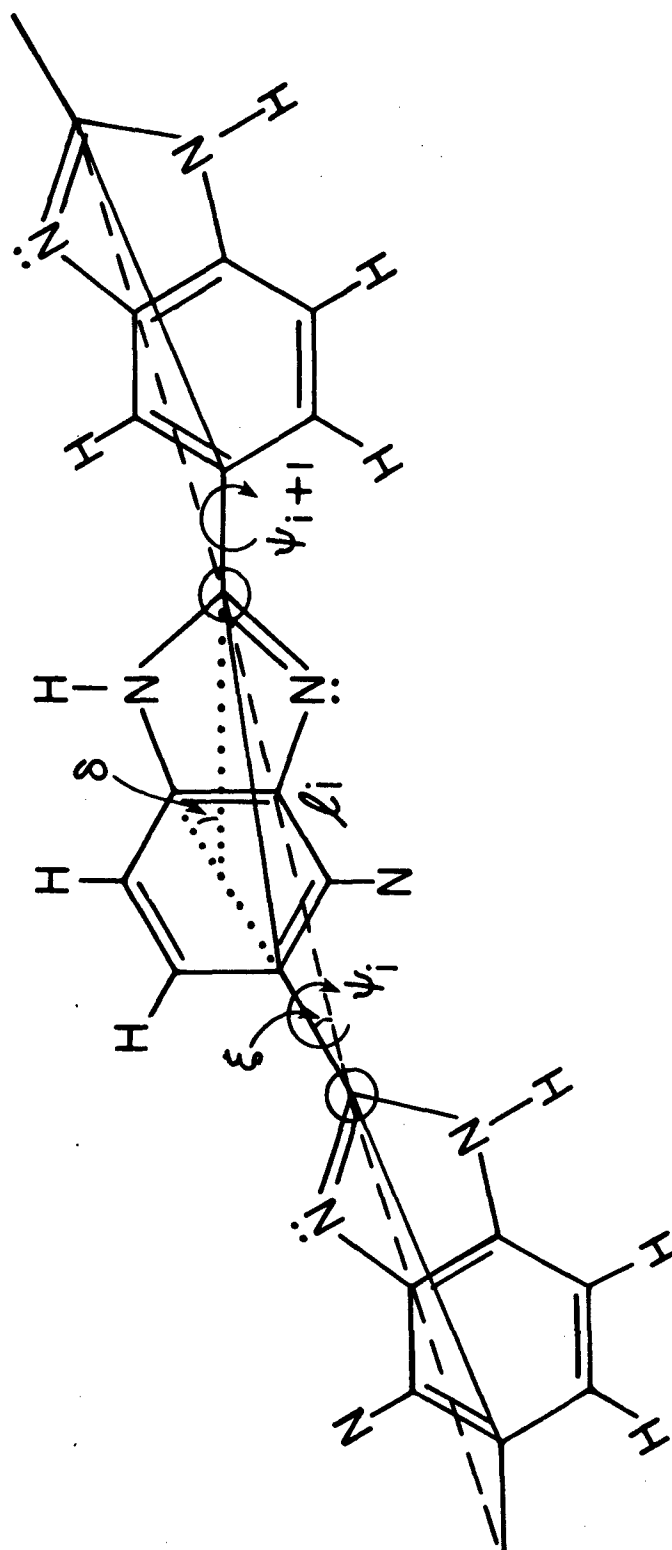


Figure 3. Schematic Representation of ABPI Chain of Fully Extended Configuration by a Virtual Bond Model, and its Geometric Parameters.

ABPBI chain possesses rather high equilibrium chain flexibility mostly due the large inherent chain bending ($\delta \approx 300^\circ$) along the chain backbone. Thus, it is unlikely for the rather long (high molecular weight) chain ABPBI molecule to sustain a rod-like conformation. That is, unless there are strong interactions between polymer and solvent molecules as discussed previously.

TABLE 1

COMPARISON OF PARAMETERS CHARACTERIZING CHAIN RIGIDITY

	AB-PBI	POLYAMIDES ^a	POLYESTERS ^a	PE ^a
$\langle X_\infty \rangle / \ell$	8.2	63	115	3.75
$\langle X_\infty \rangle, \text{\AA}$	48.6	410	740	5.75
b/ℓ	14.9	124	225	5.35
$b, \text{\AA}$	87.9	803	1450	8.20

a. P.J. Flory et al., Macromol., 13 484, 1980

In pure uncontaminated MSA and MSA/CSA mixed solvents, no liquid crystalline or spherulitic morphology was observed. Thus, in these solvents ABPBI behaves as a normal flexible coil-like polymer.

2. PHASE RELATIONSHIP OF SOLVENT/PBT/ABPBI TERNARY SYSTEMS

For each of the (97.5 MSA/2.5 CSA)/PBT/ABPBI ternary solutions investigated, there indeed existed a critical concentration point as predicted from Flory's theory (Reference 5). For all the solutions studied, when the total polymer concentration was equal to or less than the critical concentration, C_{cr} , the solution was transparent and optically isotropic. It became opaque or translucent (depending on the solution concentration) and exhibited stir-opalescence when $C > C_{cr}$. These solutions were biphasic i.e., coexistence of optically anisotropic LC domains within an isotropic phase. A typical example is shown in Figure 4a where "islands" of colored anisotropic domains (mostly green, yellow and red colors) were seen to be dispersed in a generally isotropic dark background. Figure 4b shows the influence of external

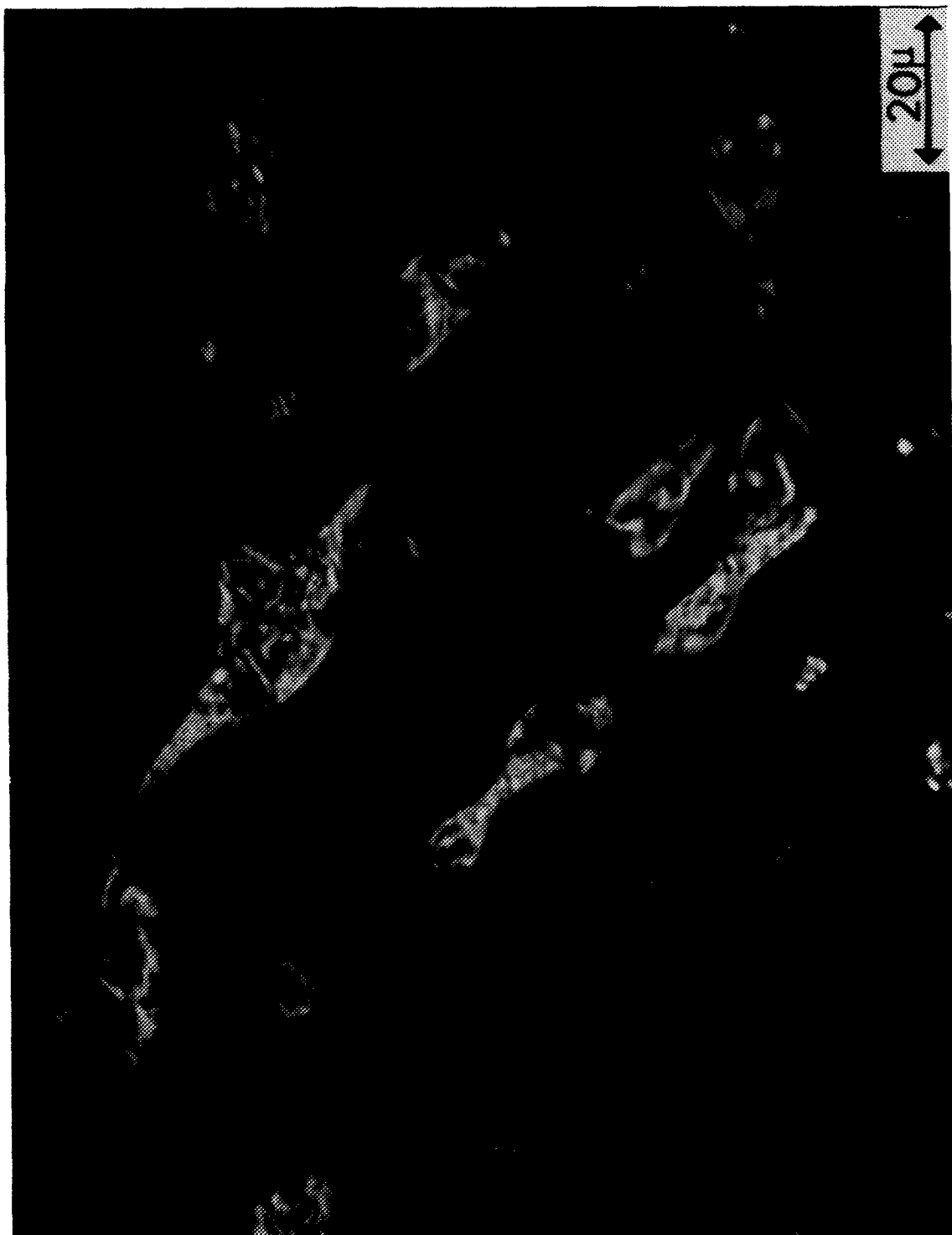


Figure 4a. OM of a Biphase Solution of 4.475 wt% 20/80 PBT (IV=18)/ABPBI in 97 MSA/2.5 CSA, Showing "Islands" of Colored Liquid Crystalline Domains Dispersed in an Isotropic Background. Crossed Nicol.

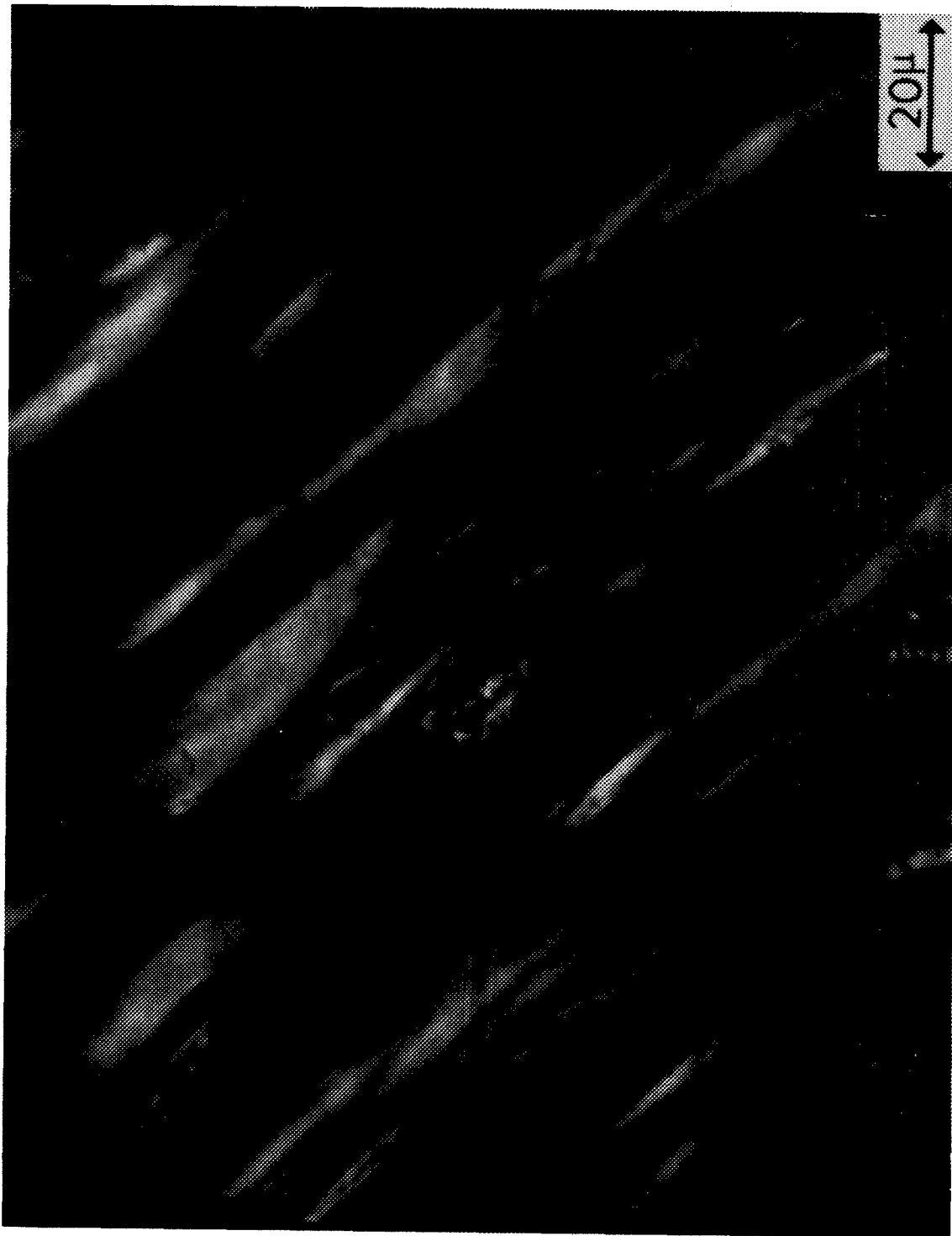


Figure 4b. OM of a Biphasic Solution (same as in (a)) Under the Influence of External Shear, Where LC Domains Are Elongated in the Shearing Direction. Crossed Nicol.

shear (sheared between glass slide and cover glass) on the solution. The anisotropic domains were generally elongated along the shearing direction (arrow direction). Examination of the retardation of these domains indicated their optical axis coincided with the shearing direction. It also indicated that molecules (in this case, the PBT molecules) inside these domains were oriented preferentially along the domain axis. As the concentration decreased, the size of liquid crystalline domains also diminished as illustrated in Figure 4c. This phase separation phenomenon in solution was observed for all the PBT/ABPBI polymer blends investigated. Undisturbed solutions (Figure 4a), did not show any common orientation among these domains. These demonstrated the nematic liquid crystalline nature of these domains.

Quenched films prepared from biphasic solution were macroscopically heterogeneous, with shiny regions seen dispersed in a generally transparent background. Figure 5 shows an optical micrograph of such an anisotropic region of a 60/40 PBT/ABPBI HSQF film prepared from 4.44 wt% ($>C_{cr}$) solution. Thread-like superstructures were seen mingled with isotropic phases. A small-angle light scattering (SALS) study of this film indicated the presence of a rod-like morphology. As shown in Figure 6, a $45^\circ H_V$ SALS pattern was observed which is indicative of individual rod-like molecules aligned preferentially along the axis of rod-like superstructures, which in turn are randomly oriented in space (Reference 19). The angle of the cross is less than 45° . This may indicate some degree of common orientation between these superstructures due to shearing (Reference 20). The $45^\circ H_V$ SALS patterns were also observed for ternary solutions in the biphasic concentration range. The OM results correlated qualitatively very well with SALS results.

For the dilute isotropic solutions ($C < C_{cr}$), and their corresponding quenched films, none of the morphological features discussed previously were observed.

Experimentally determined critical concentration points i.e., the onset of an isotropic to biphasic phase transition, and the corresponding theoretically calculated values are summarized in Table 2. They

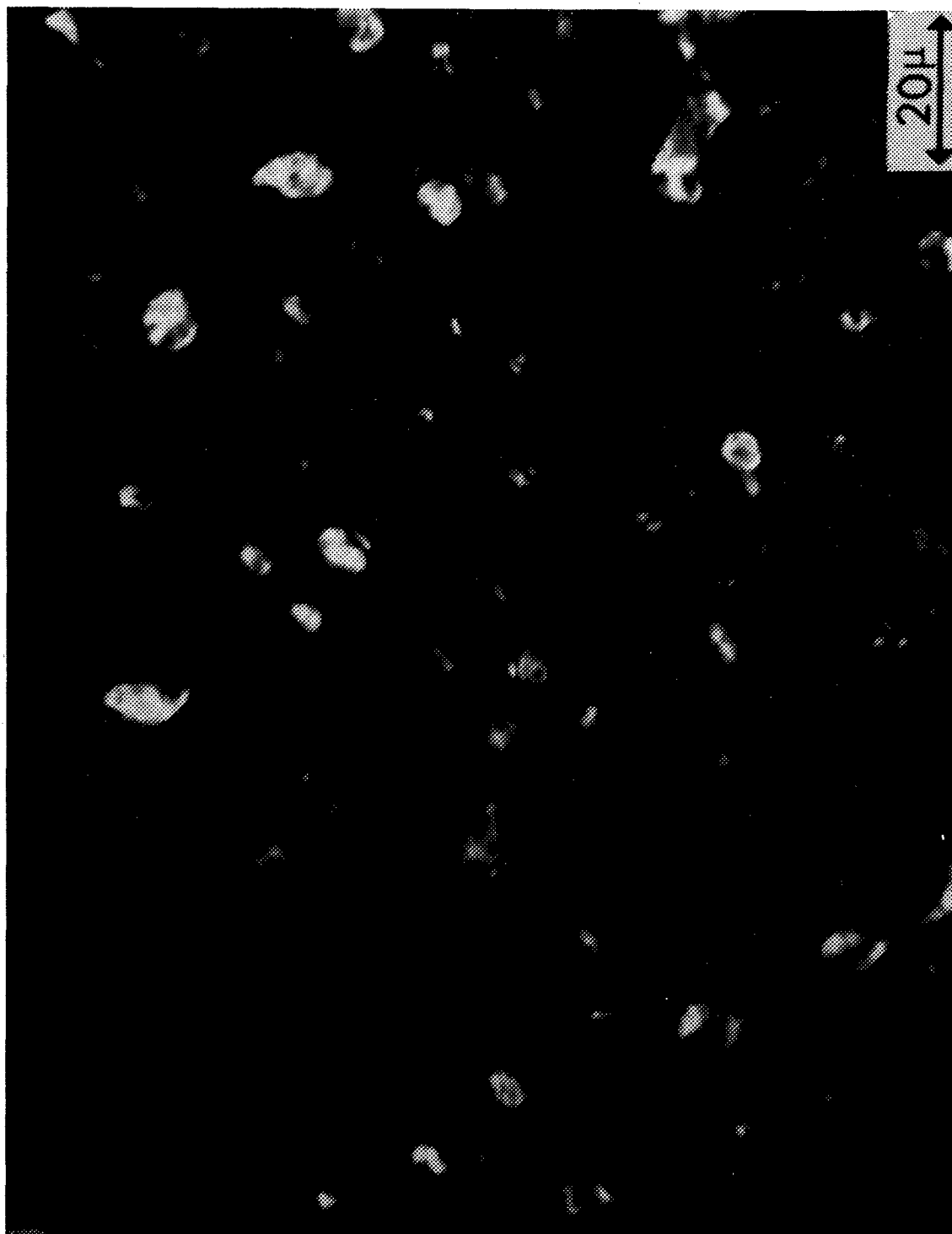


Figure 4c. OM of a Biphasic Solution of 4.35 wt% 20/80 PBT (IV=18)/ABPBI in 97.5 MSA/2.5 CSA. Size of LC domains is smaller than that in (a).

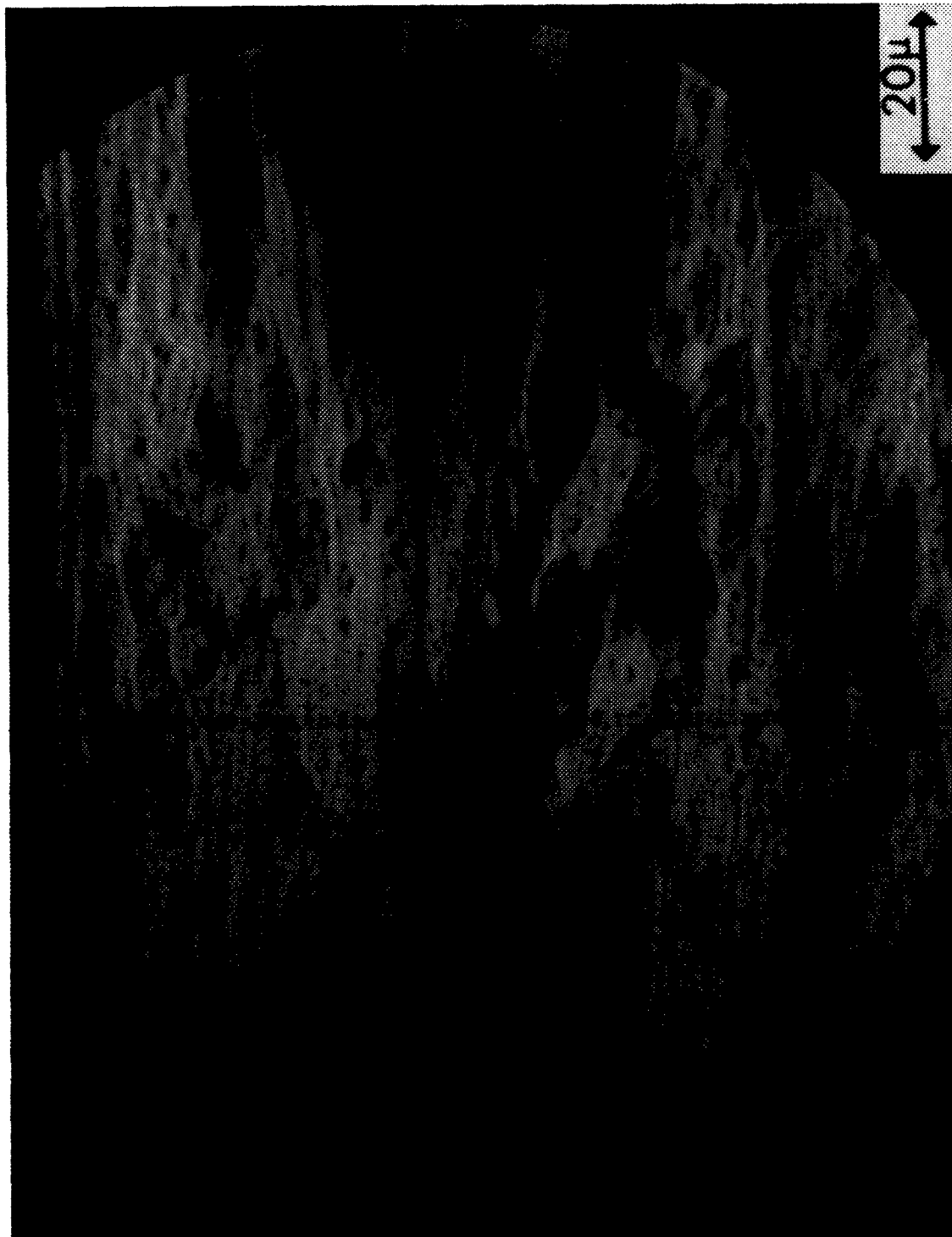


Figure 5. OM of the Mostly Anisotropic Region of an 60/40 PBT (IV=18)/ABPBI Hand-Sheared Quenched Film (HS F) from Solution with $C > C_{cr}$, Showing Distinct Rod-Like Superstructures. Crossed Nicol.

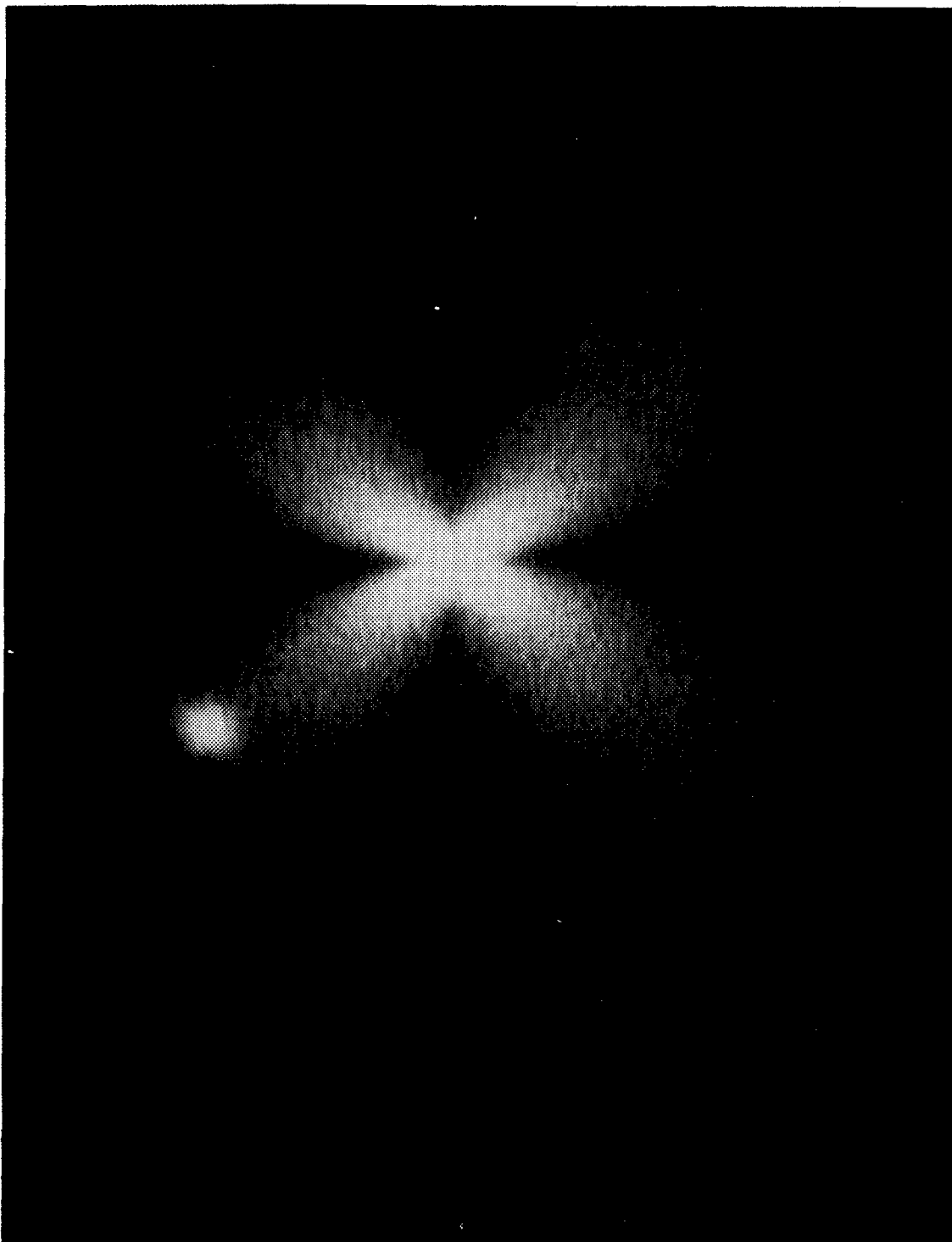


Figure 6. SALS Hv Pattern of the Optically Anisotropic Region in a 60/40 PBT (IV=18)/ABPBI HSQF. Sample to film distance = 12.5 cm.

TABLE 2
CRITICAL CONCENTRATIONS*, C_{CR} , OF ABPBI/PBT
BLENDS IN 97.5 MSA/2.5 CSA AT ROOM TEMPERATURE 22-25°C

COMPOSITION ABPBI/PBT $\left\{ \eta \right\}$ (g/dl) C_{cr}	40/60	60/40	70/30	80/20
18($X_2 = 300$)	3.00 (3.12)	3.58 (3.42)	4.05 (3.57)	4.24 (3.75)
31($X_2 = 400$)	2.50 (2.33)	2.78 (2.54)	3.05 (2.78)	3.35 (2.89)

*The experimental values are in units of wt%, while the theoretical values (in the parenthesis) are in units of vol.%. The difference between these two units is small. The density of the mixed solvent is 1.4785 g/cm³, while that for the two polymers is about 1.55 g/cm³.

are in excellent agreement with theory. The theoretical values were calculated according to the procedure outlined in Reference 5. The effective axis ratio, or aspect ratio, X_2 , for the two PBT polymers investigated (IV's 18 and 31) were estimated to be 300, and 400 from monomer unit length of 12.4 Å and width of 4.7 Å, and polymer molecular weight of 30,300, and 41,000g/mole. The effective axis ratio, X_3 , for the flexible ABPBI molecules was taken as 300. A more reasonable value would be lower because of the flexibility of the ABPBT chain. Experimental results indicated: (i) the general increase in C_{CR} as the PBT/ABPBI ratio decreased and (ii) the general decrease in C_{CR} as the molecular weight of PBT increased. A typical calculated ternary phase diagram with experimental data points is shown in Figure 7. As shown in Table 2 and Figure 7, the experimental and theoretical results were in excellent agreement. The major difference between the two was that the downward slope of the experimental isotropic binodal curve was more drastic than theoretically predicted.

The PBT/ABPBI solutions also exhibited thermotropic behavior i.e., and originally biphasic solution became totally isotropic when heated to the nematic-isotropic (biphasic to isotropic) transition temperature, T_{N-I} . The temperature-concentration phase diagrams for 40/60 and 60/40 PBT/ABPBI (IV=18 g/dl) blends are illustrated in Figure 8. They exhibit

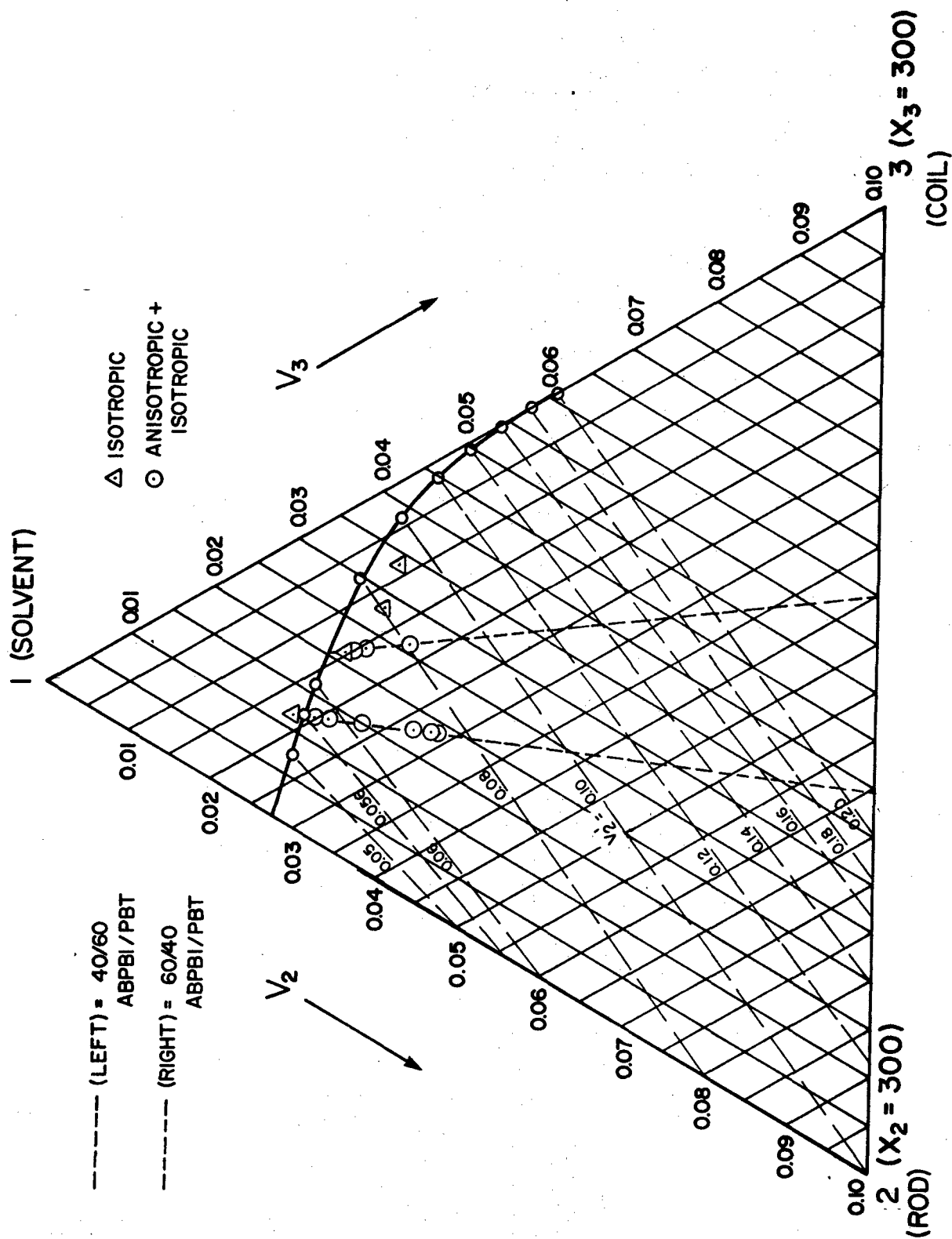


Figure 7. Calculated Ternary Phase Diagram with Experimental Data Points for Solvent/PBT (IV=18, X₂ = 300)/ABPBI (X₃ = 300) System.

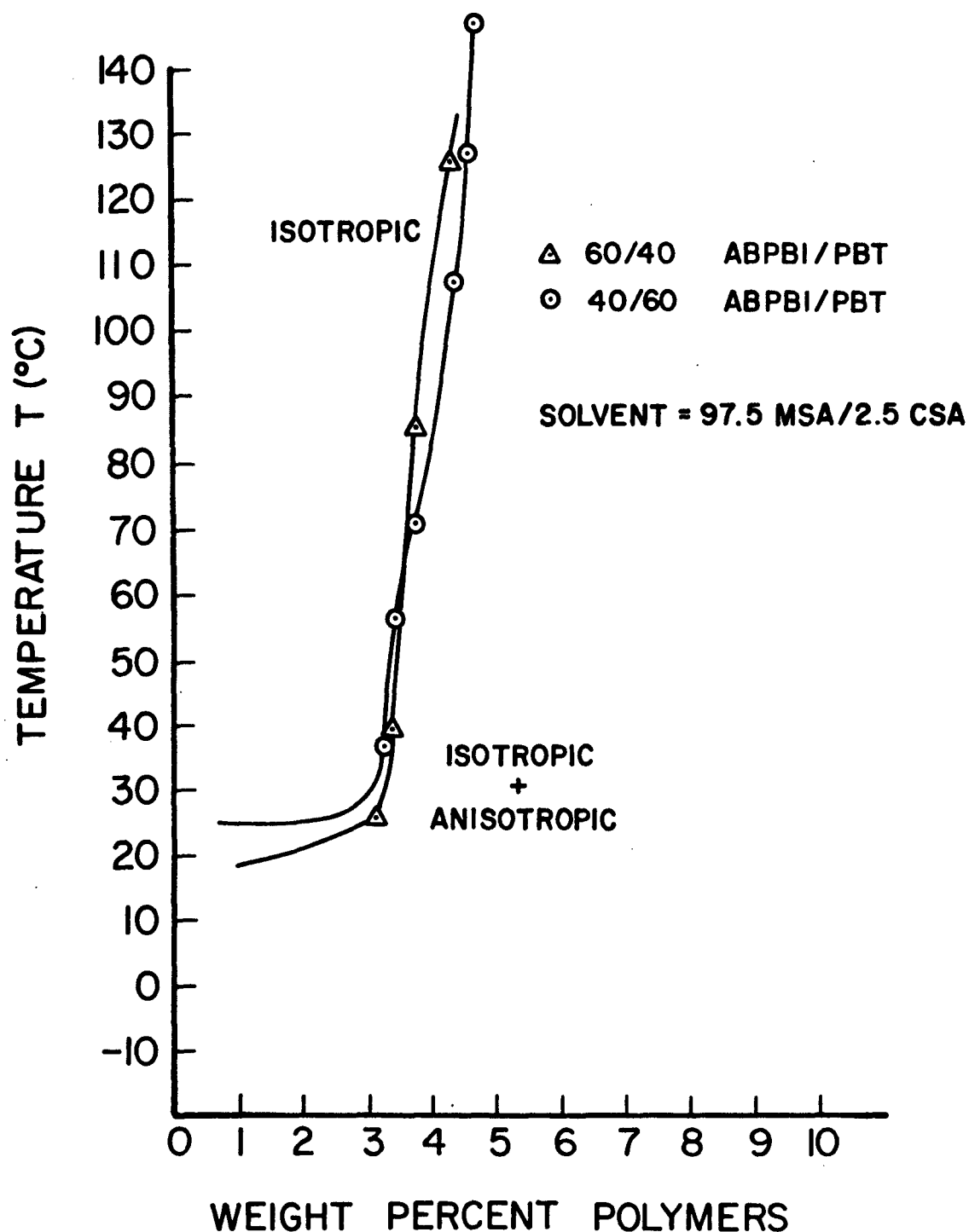


Figure 8. Temperature-Concentration Phase Diagrams for 60/40 and 40/60 PBT (IV=18)/ABPBI Solutions.

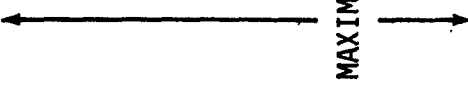
the same behavior as would be expected from a binary system containing only rod-like polymer and solvent (Reference 21).

A typical phase segregation behavior in a ternary system with $C > C_{cr}$ predicted from Flory's theory is illustrated by the data in Table 3. The calculated v_2/v_3 ratio in the isotropic phase decreases sharply as the concentration increases, while the v_3'/v_2' in the anisotropic phase stays negligibly small (10^{-4}) at all concentrations. In other words, the coil-like molecules are totally excluded from the anisotropic phase while the isotropic phase retains a nonnegligible amount of rod-like molecules. It also shows the dramatic changes in the phase composition in the two coexisting phases. A slight increase in concentration increases the total percent of rods in the anisotropic phase drastically. This in turn increases the alignment (a decrease in the disorientation factor y) of rod-like molecules inside the domain in the anisotropic phase. This accounts for the drastic increase in T_{N-I} . A quantitative determination of the composition of the two polymers in the two phases in solution would be very difficult. However, a quantified SALS study with a suitable model (References 20,22) may be fruitful for such a task.

The phase separation behavior was also manifested by the aggregate formation seen in films prepared by a vacuum casting technique (Reference 2). During slow evaporation of solvent in the casting process, the concentration, originally an isotropic dilute (2 vol %) solution, passed through its critical concentration point; and as expected, phase separation occurred. A typical SEM micrograph of the liquid nitrogen freeze-fractured surface of a cast film is shown in Figure 9. The aggregates were determined to be rich in PBT molecules by using the backscatter detector of the SEM. This enhances the phase contrast between different polymer molecules through the differences in the backscattering coefficient of electrons from different atoms. The dramatic enhancement of phase contrast of the backscattering electron image (BSEI) over the normal secondary electron image (SEI) of the SEM of vacuum cast films is clearly illustrated in Figures 10 and 11. The SEI's of aggregates of cast film surfaces can barely be seen, while the corresponding BSEI's are drastically enhanced (compare Figures 10a and 10b, 11a and 11b). Sulfur atoms, which have the highest backscattering

TABLE 3

PHASE COMPOSITIONS AND SOLUTION CHARACTERISTICS OF A 60/40 PBT(IV = 18)/ABPBI
BLEND IN 97.5 MSA/2.5 CSA AS A FUNCTION OF POLYMER CONCENTRATIONS

CONCENTRATION (WT%)	VISCOSITY* (RELATIVE)	T _{N-1} (°C)	Y	v ₂ '	(v ₂ /v ₃)*	*(v ₂ /v ₃ ')	% TOTAL RODS IN THE ANISOTROPIC PHASES**
4.74		147.6	28.90	0.074	0.359	2.13x10 ⁻⁶	76.0
4.62		126.8	29.36	0.073	0.392	2.62x10 ⁻⁶	73.9
4.40		107.2	30.83	0.070	0.463	5.34x10 ⁻⁶	69.1
3.79		70.9	35.54	0.062	0.832	3.01x10 ⁻⁵	44.5
3.43		56.5	38.54	0.058	1.146	6.82x10 ⁻⁵	23.6
3.27		36.5	39.80	0.056	1.475	9.31x10 ⁻⁵	1.7
3.00 (C _{cr})		R.T.	----	----	----	----	----
2.70		----	----	----	----	----	----
1.80		----	----	----	----	----	----

* Solution viscosity was not measured, it, however, was qualitatively determined from the observation of the stirring speed of the magnet in solution. Arrow indicated the direction of the decreases from maximum viscosity.

** Remember that the original blend has a v₂/v₃ ratio of 1.5, and all the coil-like molecules stays in the isotropic phase, so that % total in the anisotropic phase can be calculated.



Figure 9. SEI (Secondary Electron Image) of the Liquid Nitrogen Freeze Fracture Surface of a 20/80 PBT (IV=18)/ABPBI Vacuum Cast Film.



Figure 10a. SEI of the Film Surface of a 20/80 PBT (IV=18)/
ABPBI Vacuum Cast Film.

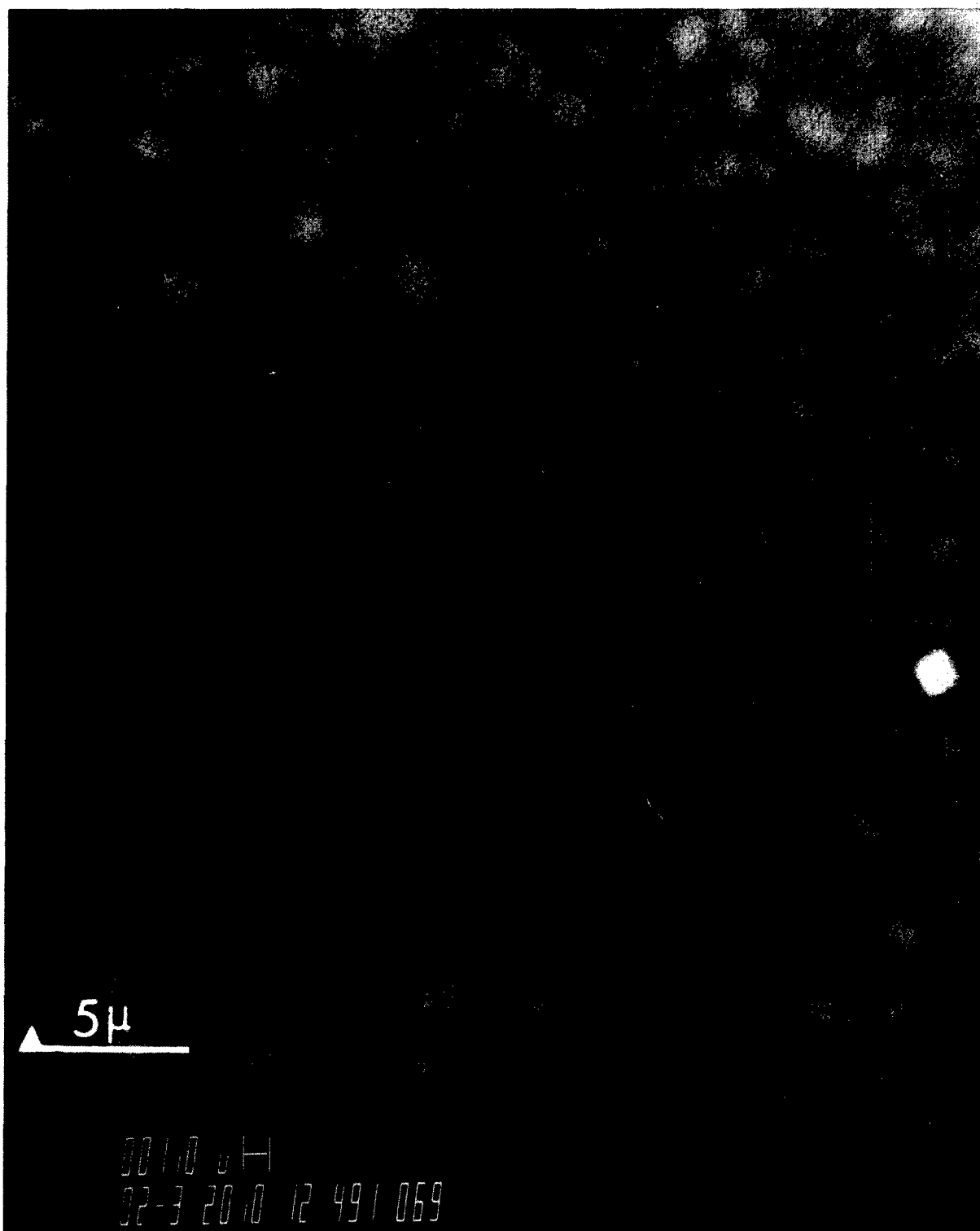


Figure 10b. BSEI (Backscattering Electron Image) of (a).

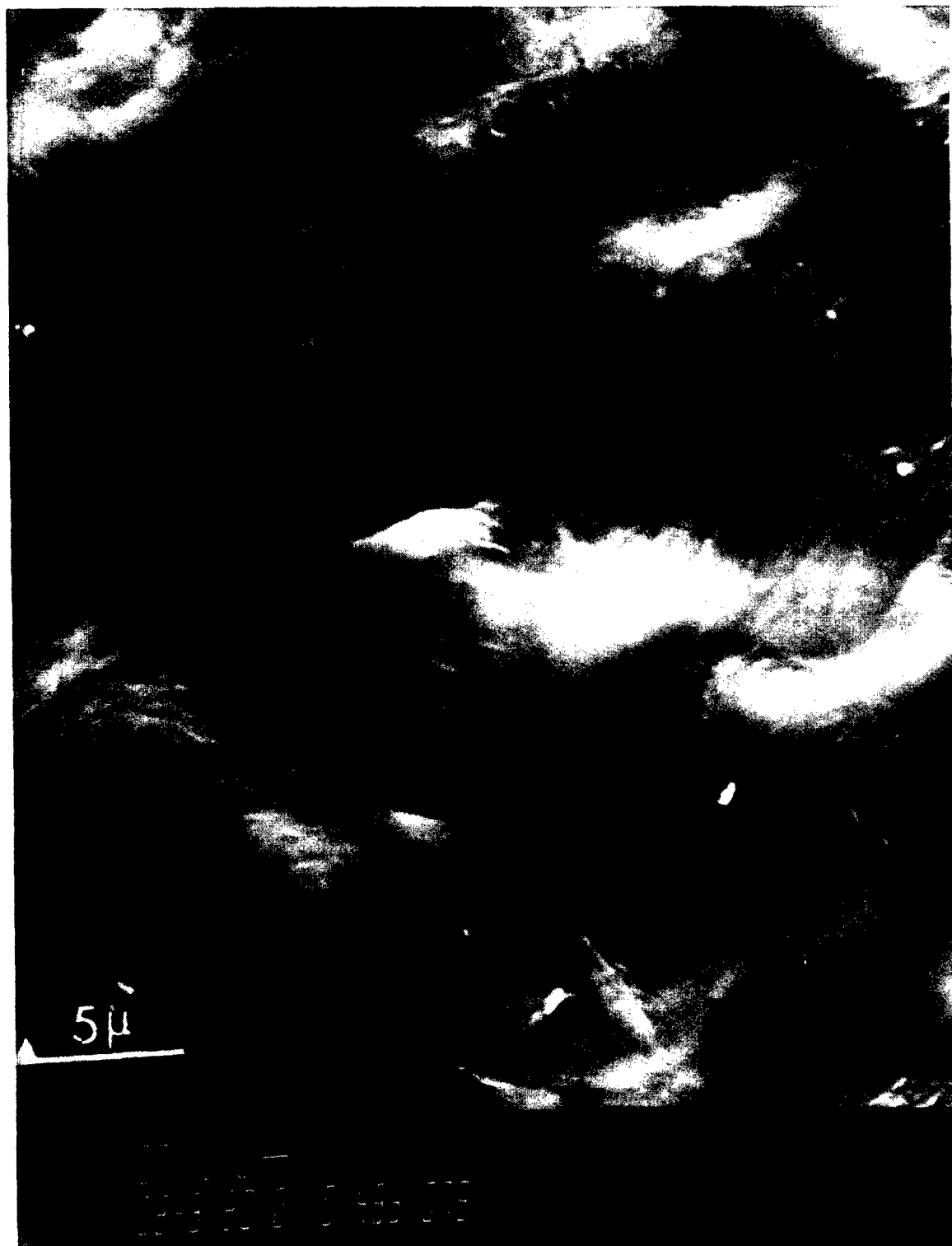


Figure 11a. SEI of the Film Surface of a 60/40 PBT (IV=18)/
ABPBI Vacuum Cast Film.

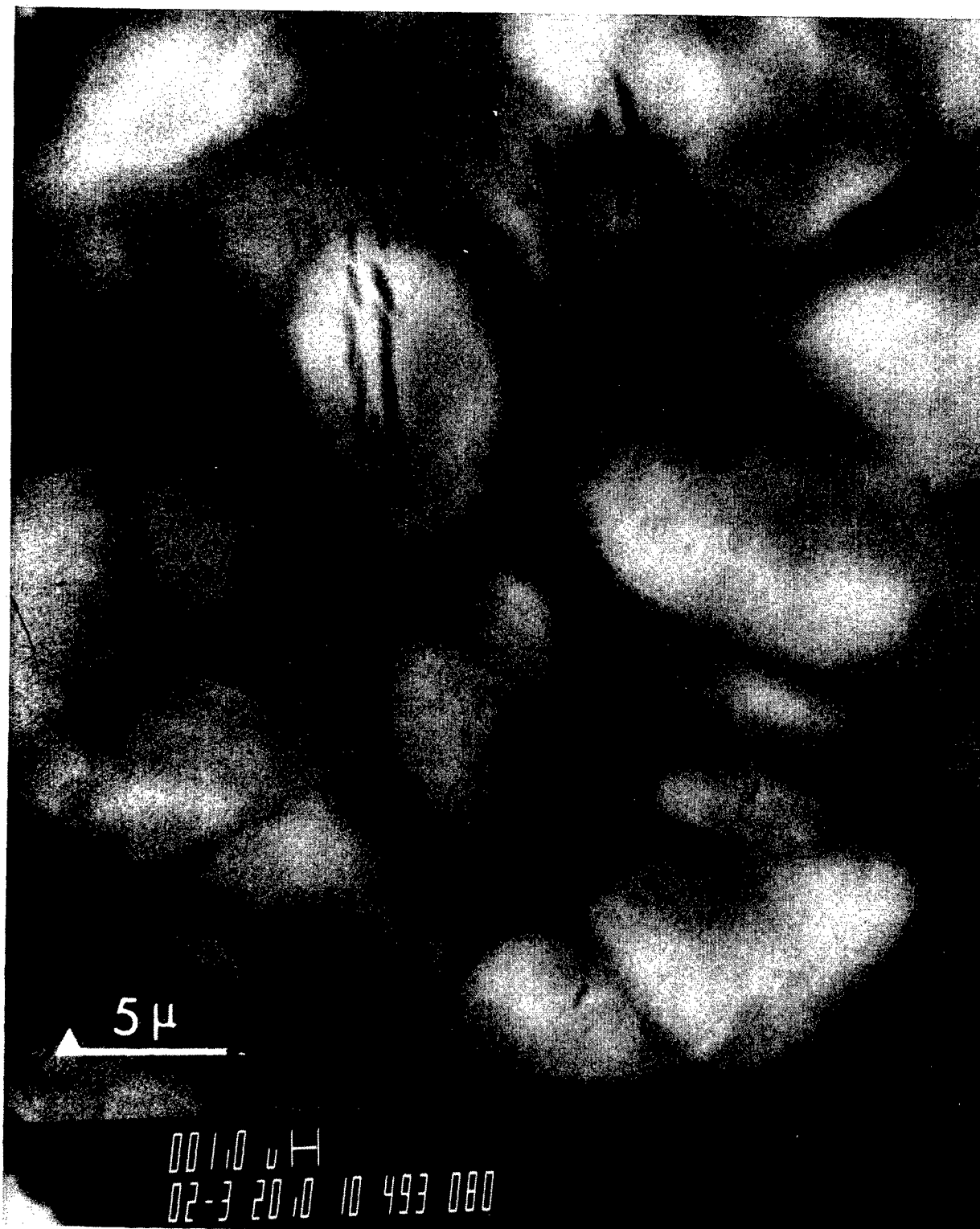


Figure 11b. BSEI of (a). Size of Aggregates is much Larger than that shown in Figure 10.

coefficient among all the atoms in ABPBI and PBT, are only present in the PBT component so that the aggregates as evidenced by the lighter domains seen in Figures 10b and 11b are composed mostly of PBT. Sharp boundaries exist between aggregates and the matrix. This is evidenced by the many holes seen throughout the matrix where aggregates had previously been located (Figure 9). Similar results were obtained for 10/90, 30/70, and 40/60 PBT/ABPBI vacuum cast films. Generally, the size of the aggregates increases as the percent composition of PBT increased. However, even at high PBT/ABPBI ratio (e.g., 60/40), phase inversion did not occur (Figure 11b). That is, the PBT molecules stayed in the dispersed phase. Considering that the molecular weight of ABPBI is much higher than PBT and the solubility of ABPBI (~ 5.5 wt%) in the 97.5 MSA/2.5 CSA solvent is much lower than that of PBT (> 12 wt%), one would expect the formation of dispersed ABPBI domains to be thermodynamically more favorable. In effect, the absence of this phase inversion phenomenon in the present polymer blends further illustrates the drastic difference in mixing behavior between the flexible coil-like ABPBI and the rigid rod-like PBT molecules. The ease for rigid rod-like PBT chains to align side by side thus segregating into space-saving nematic liquid crystalline domains is the dominant feature in these ternary systems.

The above observations in solution and in the aggregate formation seemed to suggest a total segregation between the two polymer components. Preliminary studies (Reference 23) in our laboratory using the electron energy loss spectroscopy (EELS), x-ray microanalysis, and electron diffraction also indicate that the PBT molecules are preferentially located inside the aggregates and are highly oriented.

Generally, the above results confirmed the theoretical predictions of phase segregation and high orientation of rod-like molecules inside the dispersed segregated domains. At first, the excellent agreement between our experimental results and the predictions using Flory's "athermal" lattice theory seemed surprising in light of experimental results indicating strong interactions between PBT and MSA solvent (Reference 24). This and the other possible interactions affect the enthalpy

of mixing, ΔH_m , of a polymer blend in the mixing relationship $\Delta G_m = \Delta H_m - T\Delta S_m$. However, in contrast to the usual coil-like/coil-like polymer blends, its magnitude is small as compared to the drastic change in ΔS_m resultant from the drastic reduction in the number of possible arrangements of polymer segments in a stiff rod-like chain (References 25,26) such as PBT. This is especially so for long (high molecular weight) rigid rod-like chains in a ternary system. Thus, phase relationships of (solvent/PBT/ABPBI) ternary systems appears to be governed predominantly by the large disparity in the geometry and rigidity of the two polymer molecules as pointed out in the theory (Reference 5). A similar conclusion (the dominance of entropic effects) was drawn for PBLG/PS and PHIC/PS ternary systems (Reference 27).

3. MOLECULAR COMPOSITE OF PBT/ABPBI

The phase segregation phenomenon in the present concentrated ternary solution, as discussed in the previous section, is obviously a detrimental feature in achieving our objective of obtaining a molecular level composite of PBT/ABPBI through solution processing. In retrospect, we feel that bulk molecular composites must be processed from ternary solutions at or lower than their critical concentration point via a shearing and/or elongation - quenching route. Such a process offers the advantages of high dispersion, high orientability of rigid rod-like PBT molecules in the highly viscous medium (ABPBI + solvent), and more flexibility in the processing than the vacuum casting technique. The idea is to freeze-in, through the quenching process, the high dispersity of rigid rod-like molecules in the still-isotropic solution as it is being extruded from the spinnerette or die, and subsequently elongate the partially coagulated solution to achieve orientation. Since one of the main purposes of this report was to demonstrate the feasibility of obtaining a molecular level composite of PBT/ABPBI, we show the results on the processing, properties, and characterization of a (30/70) PBT/ABPBI composite fiber as an illustrating example. Implications from it will certainly hold for other bulk forms such as films.

The solution spinning process and tensile testing method were described in detail in the experimental section. (30/70) PBT (IV = 31)/ABPBI composite and pure ABPBI fibers were processed at identical conditions from a 2.5 wt% solution. In the 30/70 blend case this is lower than its critical concentration. The average diameters for as-spun composite fibers and pure ABPBI fibers are 2.4 mil (2.4×10^{-3} inch) and 1.5 mil, respectively. The difference in the measured diameter can be attributed to the fact that ABPBI solution (same concentration as that of the 30/70 blend) is less viscous than the 30/70 blend, so that the initial draw-down (by gravity) between the spinnerette and the first water bath is more for the ABPBI solution than for the blend solution.

Results of uniaxial tensile testings and descriptions of these fibers are summarized in Table 4. The last column in Table 4 represents the back-calculated uniaxial Young's modulus, E_f , for PBT from experimentally determined modulus for ABPBI matrix (E_m) and 30/70 PBT/ABPBI composite (E_{11}) according to the rule of mixture i.e., $E_f = (E_{11} - v_mE_m)/v_f$. The best experimentally determined (Reference 28) value for pure PBT fiber to date was 42 million psi as compared to our back-calculated values of 35-44 million psi. Thus, from the mechanics of composites viewpoint we have indeed obtained, at least in the cases of NHT977 and NHT1010, a composite which has apparently fully utilized the modulus of the reinforcing constituent. This conclusion is based on the validity of the rule of mixtures. The calculations are based on the presumption of a complete dispersion and perfect orientation of individual PBT molecules, having respective aspect ratios (ζ) of 600 and 800. However, it should be noted here that in the event of phase separation or crystalline formation during the high temperature heat treatment the total volume fraction of the individual fully extended PBT molecules would decrease. As a result, the effective aspect ratio would be less and thus the back-calculated PBT modulus would be too low. The effect of the aspect ratio of the PBT phase on the uniaxial modulus of the (30/70) PBT/ABPBI is illustrated in Figure 12 (see Equations 1, 2, and 3). As shown in Figure 12, in order for the uniaxial modulus of the (30/70) PBT/ABPBI NHT1010 composite fiber to reach 98% of its upper

TABLE 4
DESCRIPTION AND TENSILE PROPERTIES*
OF 30/70 PBT (IV = 31)/ABPBI BLEND AND
ABPBI FIBERS**

COMPOSITION & DESIGNATION***	FURTHER DRAW RATIO DURING HEAT TREATMENT	YOUNG'S MODULUS, E_m E_{11} , (x10 ⁻⁶ PSI)	TENSILE STRENGTH TS, (x10 ⁻³ PSI)	ELONGATION AT BREAK, (%)	BACK CALCULATED PBT MODULUS, E_f (x10 ⁻⁶ PSI)****
ABPBI- AS	-	2.09 (2.43)	96.56 (97.90)	28.15 (29.60)	-
ABPBI- NHT977	1.20	4.44 (5.00)	157.10 (168.30)	6.60 (7.20)	-
ABPBI- NHT1010	1.20	5.27 (5.75)	157.65 (170.57)	5.23 (5.70)	-
30/70- AS	-	4.83 (4.91)	134.10 (136.30)	6.50 (6.80)	11.22
30/70- NHT800	1.10	9.93 (10.40)	172.30 (176.20)	2.43 (2.46)	-
30/70- NHT977	1.20	13.60 (15.9)	186.10 (218.60)	1.67 (1.80)	35.00
30/70- NHT1010	1.20	16.90 (17.45)	184.10 (197.60)	1.41 (1.61)	44.04

* Average of four testings. Values in parenthesis indicate best property.

** All the fibers had initial draw ratio of 3.4. Draw ratio = $\left(\frac{D_o}{D_I}\right)\left(\frac{RS_o}{RS_I}\right)$; D is diameter of roller RS the roll speed; subscripts o and I represent output and input roller, respectively.

*** AS=as spun, HT=heat treatment, N=neutralized in NH₄ H, Numbers (such as 800, 977, etc) indicate temperature of heat treatment in °F.

**** From rule of mixtures.

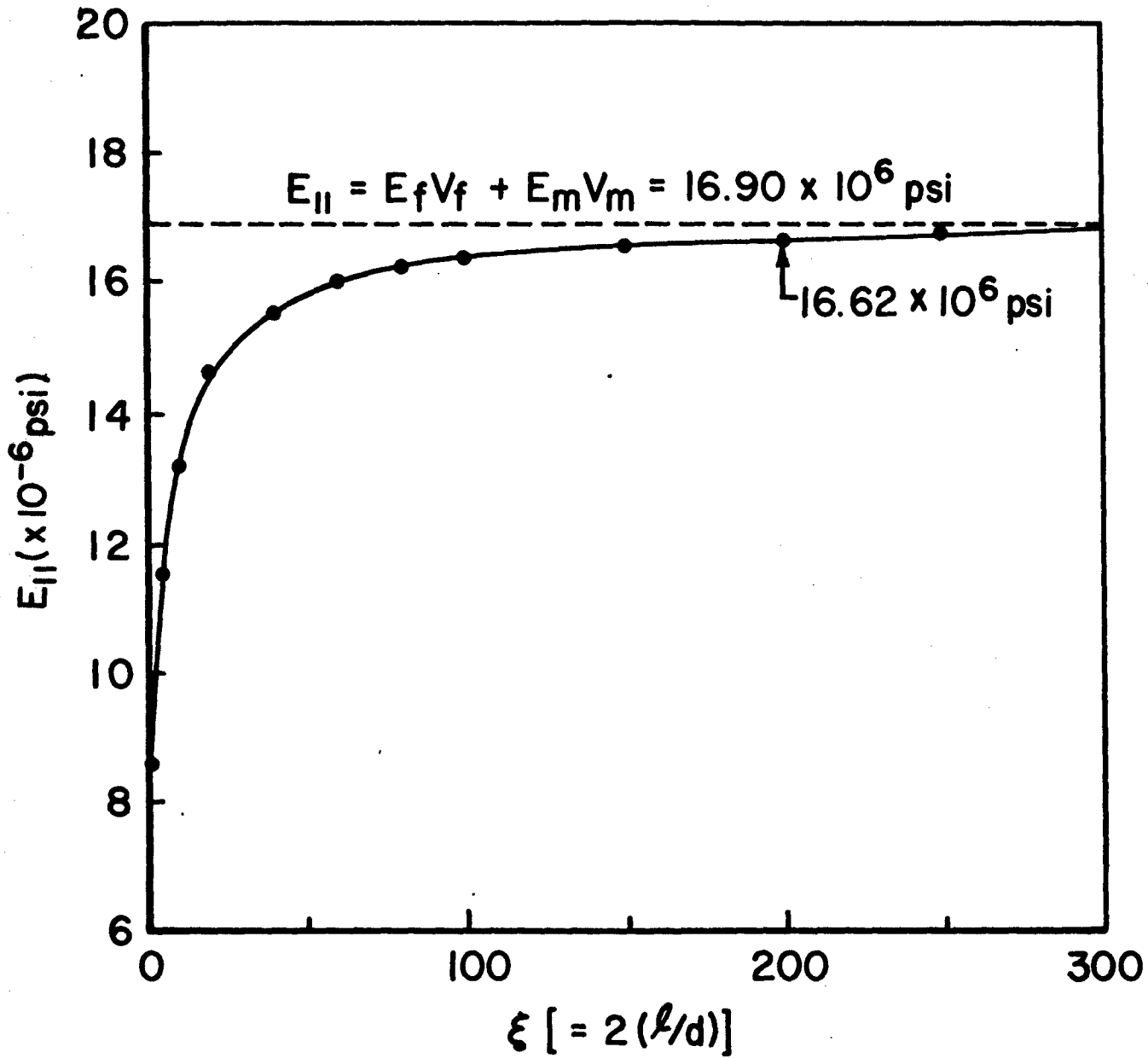


Figure 12. Uniaxial Modulus, E_{II} of 30/70 PBI (IV=31)/ABPBI NHT1010 Composite as a Function of Aspect Ratio, ξ .
 $E_f = 44$ MSI, $E_m = 5.2$ MSI.

bound limit value ($E_{11} = v_v E_f + v_m E_m$), the aspect ratio of the PBT phase has to be at least 100 ($\zeta = 200$). Furthermore, as shown in Table 4, one can easily "tune" the composite to a desired set of properties (modulus, strength, elongation), through the variations in the solution processing and post-treatment conditions. Experimental results on the characterization of the observable phase structure, if any, of (30/70) PBT/ABPBI fibers by SEM and WAXD method, are presented in the next section.

Figure 13 shows the SEM of a tensile broken (30/70)PBT/ABPBI NHT1010 fiber. It clearly exhibits an extremely fibrillar morphology. As shown in Figure 14, except for the observed surface features, examinations using the backscattering detector of the SEM on the internal surface of a split virgin 30/70 PBT/ABPBI NHT1010 fiber did not reveal any discernible subsurface structures or domains as those observed in Figures 10 and 11. The absence of a second phase in the SEM of PBI/ABPBI composites is universal among all the bulk specimens processed from ternary solutions at $C < C_{cr}$. It should be noted here that the domain (or phase) resolution of the SEM in the backscattering mode is 0.1 microns. Thus, these SEM results only indicate that the size of the second phase, if present, in the bulk specimen is small ($< 1000\text{\AA}$).

The elucidation of microphase structures of composite and pure ABPBI fibers is better served by wide-angle x-ray diffraction (WAXD) technique; since it probes the molecular level. The crystalline structure of pure PBT fiber has been extensively studied (References 29,30). Both WAXD and electron diffraction studies on specimen showed two strong equatorial reflections with corresponding d-spacings of 5.9 Å and 3.5 Å. The meridional reflections (00ℓ) were determined to correspond to a fiber repeat unit of 12.35 Å. The WAXD pattern of a ABPBI-NHT1010 fiber is shown in Figure 15. It shows two characteristic equatorial d-spacings of 7.0 Å and 3.5 Å. The meridional reflections (00ℓ) corresponds to a fiber repeat distance of 11.5 Å, which relate to the length of two monomer units of an ABPBI chain in its extended chain conformation. It should also be noted that the ABPBI-NHT1010 fiber has a higher crystalline order than pure PBT fibers. This is evidenced by the presence of higher-order ($hk\ell$) reflections which were absent in pure PBT

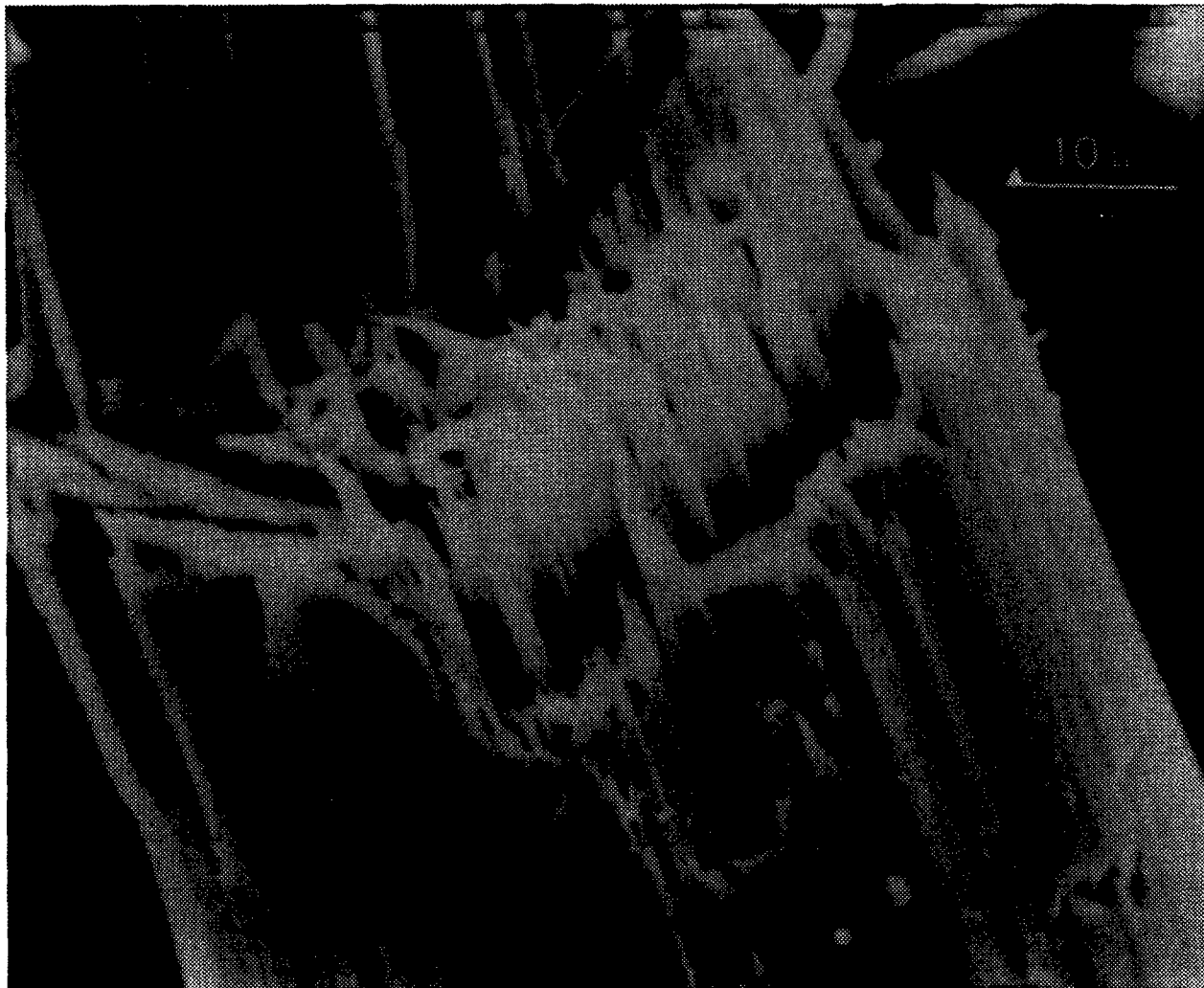


Figure 13. SEI of a Tensile Broken 30/70 PBT (IV=31)/ABPBI NHT1010 Composite Fiber.

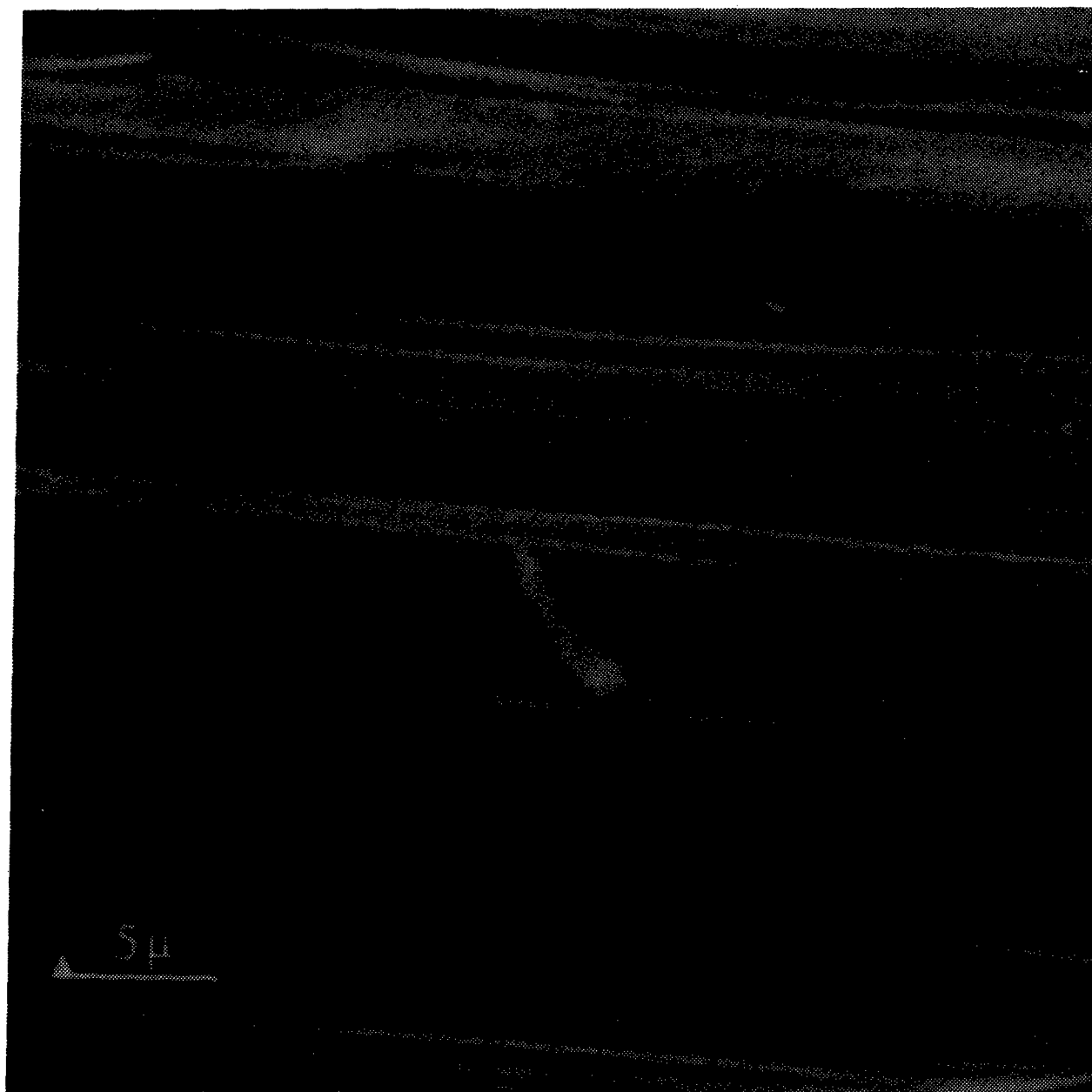


Figure 14a. SEI of the Internal Surface of a Peeled 30/70 PBT (IV=31)/ABPBI NHT1010 Composite Fiber.

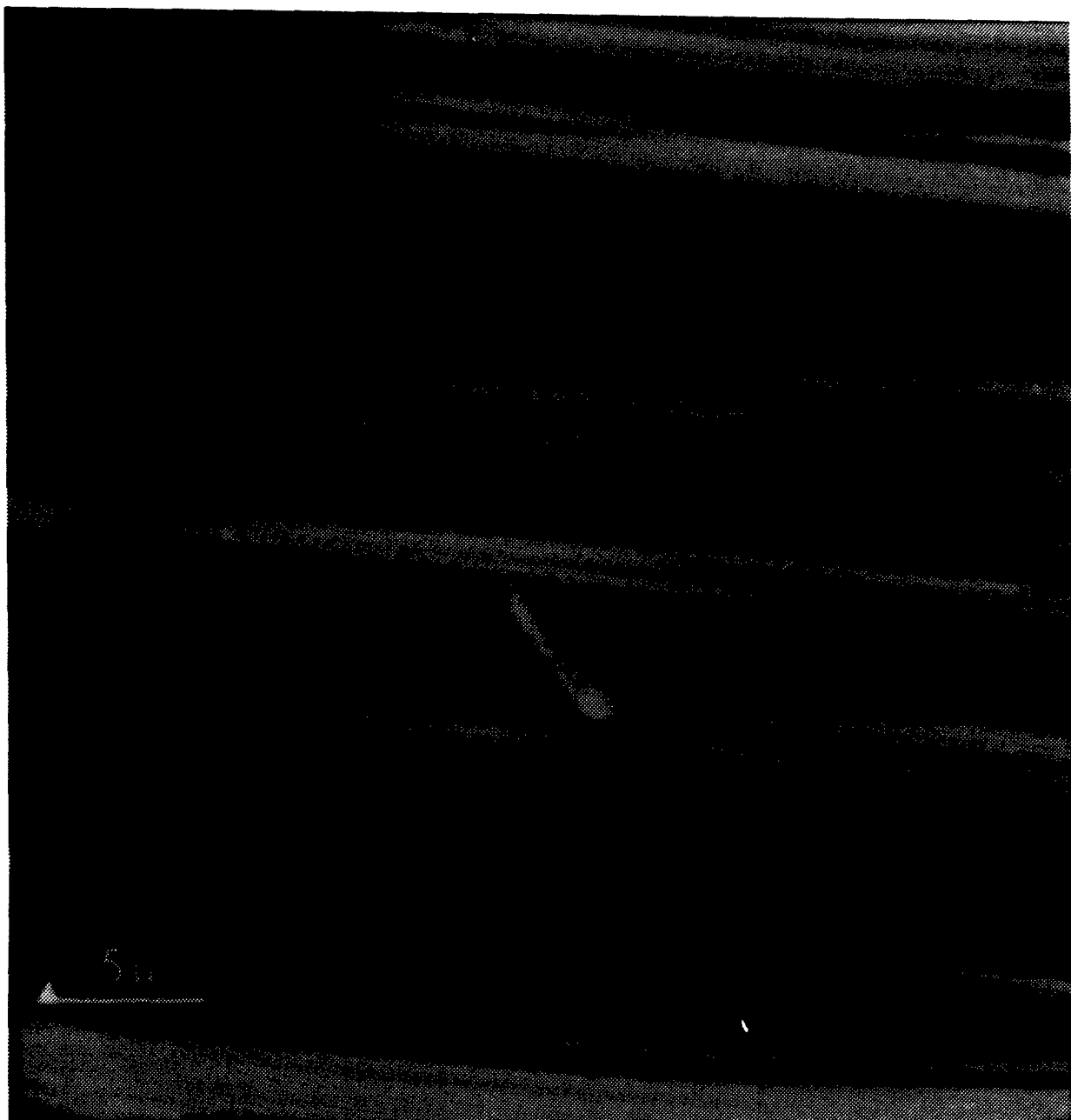


Figure 14b. BSEI of (a).

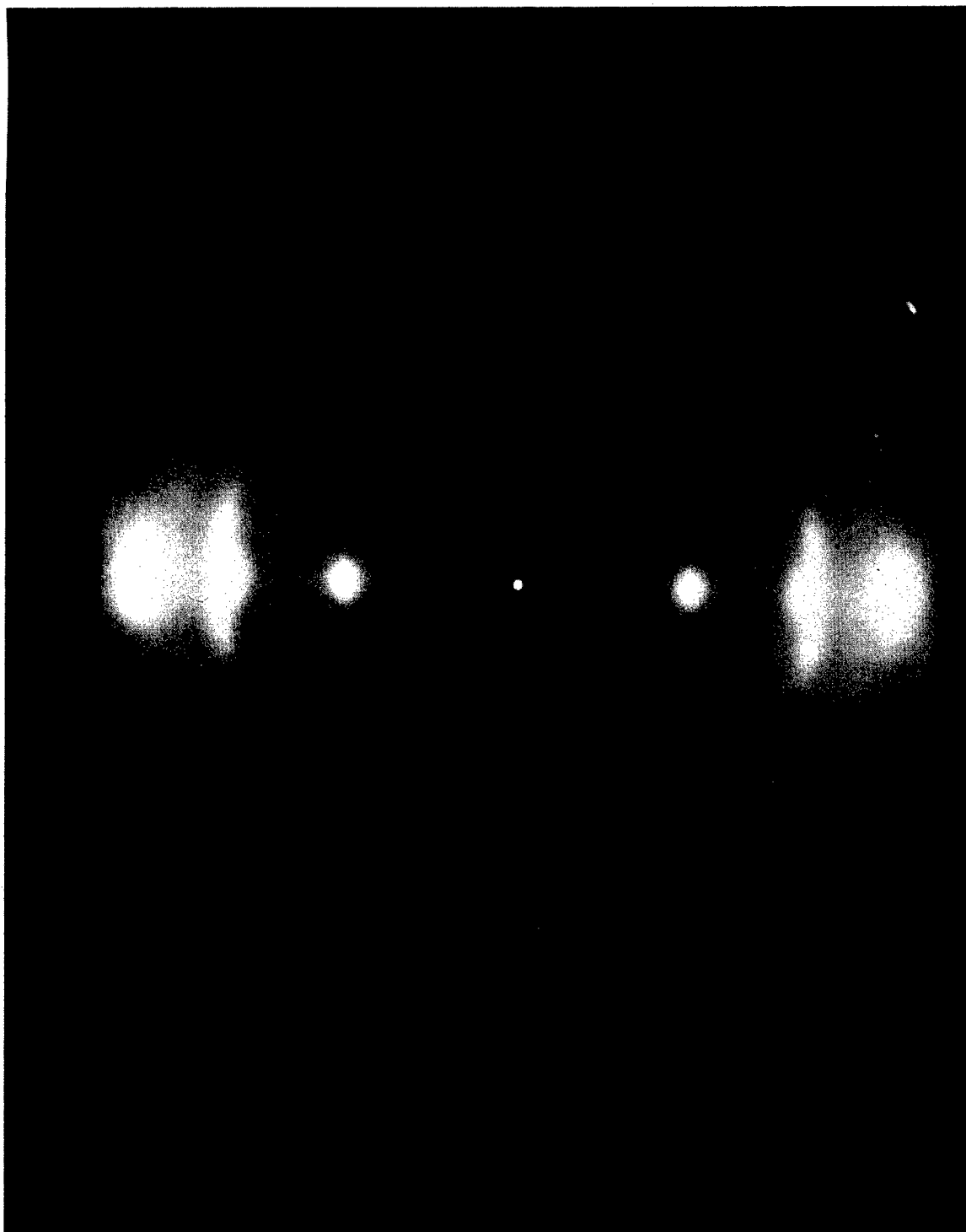


Figure 15. WAXD of ABPBI NHT1010 Fiber 8 Filaments. Norelco 40kv 20 MA. 168 hrs exposure.

WAXD patterns. Furthermore, some reflections e.g., the first and third meridional reflections are split. This is another strong indication that in contrast to PBT molecules, an ABPBI chain does not have a straight rod type conformation even in the highly elongated state; rather it has a zig-zag twisting helical coil-like conformation as previously indicated. In the as-spun ABPBI fiber, the first strong and rather diffuse equatorial reflection has a corresponding 7.8 \AA d-spacing as compared to 7.0 \AA in the ABPBI-NHT1010 fiber. In the as-spun fiber the lattice is swollen by residual MSA molecules, so that it has a larger lateral d-spacing (7.8 \AA) than that of a solvent-free high temperature heat treated fiber. As a rule of thumb, this spacing varies from 7.8 \AA in the as-spun fiber, 7.4 \AA in the neutralized fiber, to 7.0 \AA in the high temperature (977°F and 1010°F) heat treated fiber. This variation is also reflected in the corresponding 30/70 PBT/ABPBI composite fibers. The WAXD pattern of an as-spun 30/70 PBT/ABPBI fiber is shown in Figure 16a. Only the swollen 7.8 \AA and the ever-present 3.5 \AA d-spacings characteristic of pure ABPBI are present in the equator; while a superposition of (00ℓ) reflections corresponding to both ABPBI and PBT are observed along the meridian. As shown in Figure 16b, the heat treatment did bring about microphase-separation in the 30/70 PBT/ABPBI NHT1010 fiber. A possible explanation for this will be presented below. Both the 7.0 \AA (ABPBI) and 6.0 \AA (PBT) d-spacings are observed on the equator, and superposition of (00ℓ) reflections of both components are observed. Both phases are highly crystalline and oriented. Higher-order (hkl) reflections observed in ABPBI-NHT1010 fiber are absent in this 30/70 PBT/ABPBI NHT1010 fiber. In summary, the above WAXD results indicate the following: (1) The superposition of the characteristic PBT meridional (00ℓ) reflections on the characteristic ABPBI meridional reflections in both the as-spun and NHT1010 composite fibers indicates that rigid rod-like PBT molecules are highly oriented along the fiber axis, irrespective of lateral (positional) order; (2) The above also strongly points out the extremely high rigidity possessed by PBT molecules; (3) The absence of the 6.0 \AA equatorial d-spacing characteristic of PBT (see Figure 16a) in the as-spun 30/70 composite fiber, coupled with the assurance of high dispersity (one can argue that some of the largest PBT molecules may have already segregated out of the isotropic solution) indicate that the PBT molecules are molecularly dispersed in the ABPBI matrix; (4) The presence of the

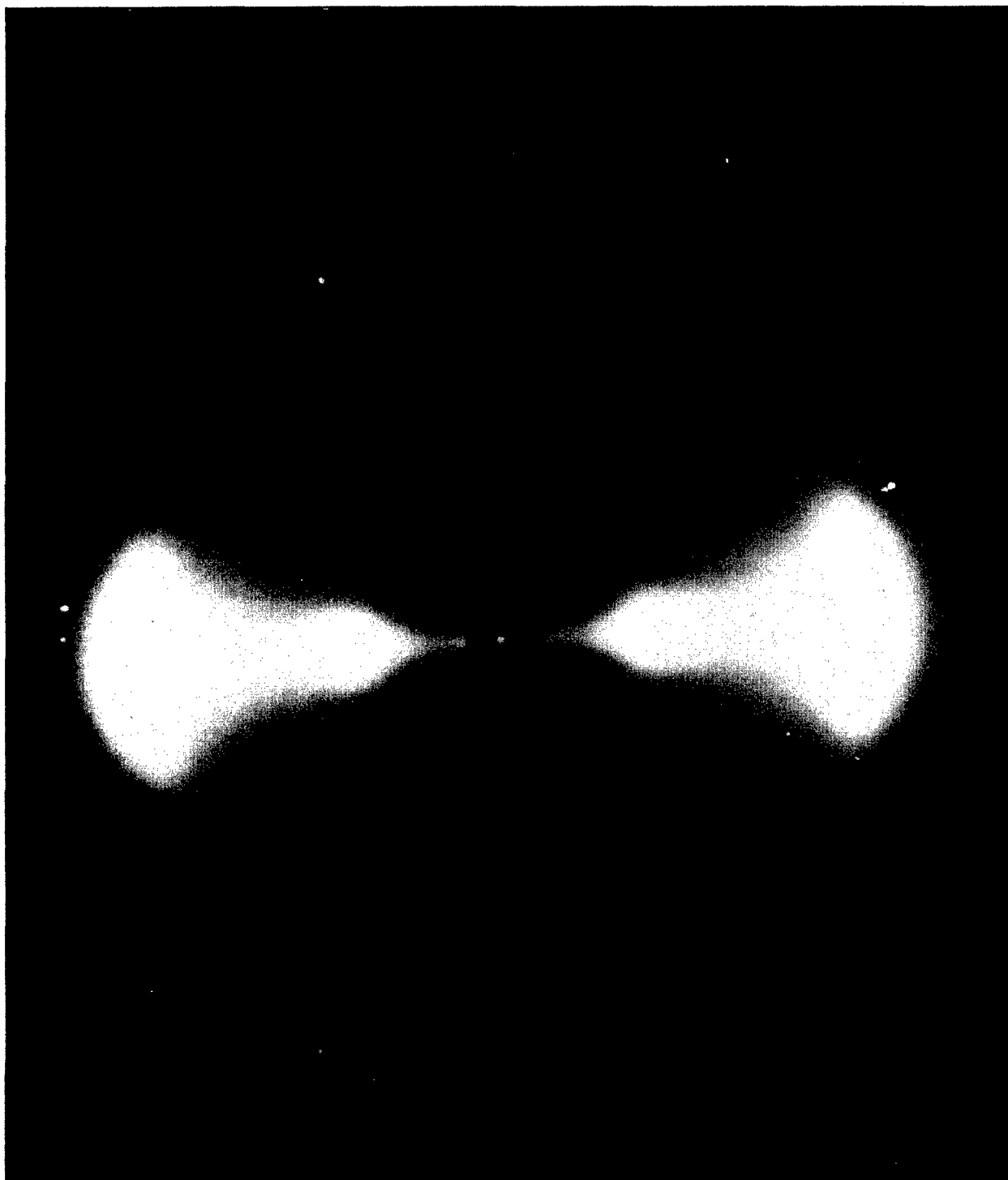


Figure 16a. WAXD of As-Spun 30/70 PBT (IV=31)/ABPBI Composite Fiber, 8 Filaments. Norelco 40kv 20MA, 168 hrs exposure.

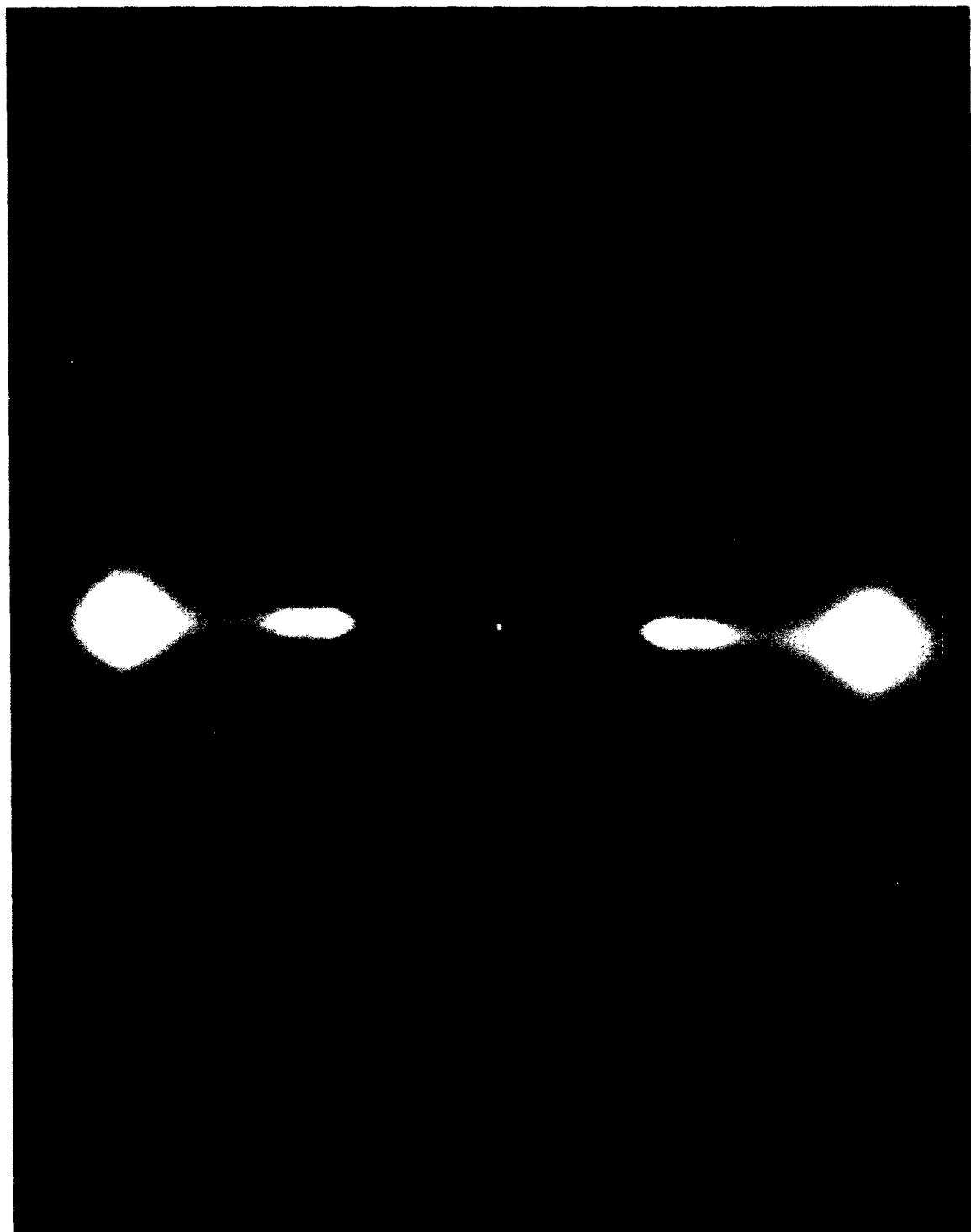


Figure 16b. WAXD of 30/70 PBT (IV=31)/ABPBI NHT1010 Composite Fiber.
8 Filaments, Norelco 40kv 20MA, 168 hrs exposure.

6.0 Å (PBT) d-spacing in the 30/70 NHT977 and NHT1010 composite fibers indicates the possible formation of PBT crystallites. This indicates the presence of domains rich in PBT molecules. More important, the presence of this may simply indicate that the crystalline lattice of ABPBI has been altered by the PBT molecules; (5) In light of the dark field - electron microscopy results for pure PBT, the size of the above mentioned PBT crystallites in the 30/70 NHT1010 composite fiber would be very small e.g., 60 to 80 Å in width and 300 to 400 Å in length for pure PBT fibers; (6) The observed 7.0 Å (ABPBI) and 6.0 Å equatorial peaks in the 30/70 NHT1010 fiber are qualitatively broader than that in the corresponding pure homopolymers (compare Figure 16b and Figure 15); (7) The observation in item (6) coupled with the observed absence of higher order ABPBI (hkl) reflections in the 30/70 NHT1010 composite fiber indicate strong (intimate) mutual disturbance in the crystalline order between PBT and ABPBI crystallites; (8) The heat treatment temperatures (977°F, 1010°F) of the composite fibers were very far from the conceptual T_m (>1500°F) of both ABPBI and PBT homopolymers, therefore, the percentages of PBT and ABPBI molecules segregated into respective crystallites would be expected to be very small.

From the above results and discussions, we can safely conclude that the as-spun 30/70 PBT/ABPBI fiber is indeed a molecular level composite. Its failure to fulfill the rule of mixtures for individual modulus is simply reflected from the lack of perfect orientations of PBT molecules along the fiber axis. In the cases of 30/70 PBT/ABPBI, NHT977 and NHT1010 fibers, the number of tiny segregated PBT crystallites with very low aspect ratio is simply too small (as compared to those individually dispersed PBT molecules) to affect the fulfillment of the rule of mixtures for their uniaxial modulus. Further morphological characterization (using small-angle x-ray scattering, electron diffraction, and high resolution STEM techniques), and quantitative analysis of orientation and crystalline/amorphous composition (using microdensitometry of WAXD patterns and birefringence measurements), in relation to mechanical properties of these bulk specimens are currently underway. These results will be reported later.

SECTION IV

CONCLUSIONS

Agreement between theoretical conformation analysis, chain statistics, and observed solution behavior of ABPBI polymer indicates it has a high equilibrium chain flexibility to assume a flexible coil-like configuration in an uncontaminated 97.5 MSA/215 CSA or MSA solvent. The solvent/rigid rod-like PBT/flexible coil-like ABPBI ternary systems has been established. Excellent agreement between the experimentally observed phase behavior of these ternary systems and Flory's theory strongly indicates the dominance of entropic effects in the mixing behavior of PBT/ABPBI in a common solvent. The inevitability of phase segregation between PBT and ABPBI in ternary solution at $C > C_{cr}$ is a detrimental feature in processing these mixtures into useful products at normal room conditions. The underlying basis, as inferred through the establishment and understanding of the phase relationship of these ternary systems, for the actual solution processing is demonstrated.

Results from WAXD and SEM characterization of the morphology, and from the composite micromechanics analysis on the uniaxial modulus, of the composite fiber strongly indicates the attainment of the molecular level composite (or very close to it) of highly dispersed, oriented PBT molecules in an ABPBI matrix.

The concept of a molecular composite of rigid rod-like/flexible coil-like polymer blends has for the first time been validated. The results of this investigation have obvious implications with reference to the solution processing of other similar rigid rod-like flexible coil-like polymeric blends into "molecular composite", either in fiber or film form.

REFERENCES

1. T. E. Helminiak, et. al., "Aromatic Heterocyclic Polymer Alloys and Products Produced Thereby", U.S. Patent Appl. S/N 902, 525 (1978).
2. G. Husman, T. Helminiak, W. Adams, D. Wiff, and C. Benner, ACS Organic Coat. and Plast. Chem., 40, 797, (1979)
3. M. Wellman, G. Husman, A.K. Kulshreshtha, T. Helminiak, D. Wiff, C. Benner, and W.F. Hwang, Ibid, 43, 783 (1980).
4. J. L. Kardos and J. Raison, Polym. Engineer and Sci., 15, 183 (1975).
5. P. J. Flory, Macromol., 11, 1138 (1978).
6. P. J. Flory and A. Abe, Macromol., 11, 1119 (1978).
7. S. M. Aharoni, Polymer, 21, 21 (1980).
8. S. Diner, J. P. Malrieu, F. Jordan, and M. Gilbert, Theor. Chim. Acta., 15, 100 (1969).
9. E. Erman, P. J. Flory, J. P. Hummel, Macromol., 13, 484 (1980).
10. C. B. Delano, R. R. Dole, and R. J. Milligan, AFML-TR-74-22, (1974).
11. G. C. Berry, E. F. Casassa, P. Metzger, and S. Venkatramen, AFML-TR-78-164, April (1979).
12. T. E. Helminiak, ACS Org. Coat. and Plast. Chem., 40, 475 (1979); G. C. Berry, C. P. Wong, S. Venkatramen, and S. G. Shu, AFML-TR-79-4115, August (1979).
13. T. Kojima, Polymer J., 12, 85 (1981).
14. T. S. Hanley, T. E. Helminiak, and C. L. Benner, J. Appl. Polym. Sci., 22, 2965 (1978).
15. S. M. Aharoni, J. Appl. Polym. Sci., 21, 181 (1977).
16. M. C. J. Dik-Edixhoven, H. Schenk, and H. VanderMeer, Cryst. Struct. Comm., 2, 23 (1973).
17. M. V. Volkenstein, "Configurational Statistics of Polymer Chains", Chap. 4, Interscience, (1963).
18. P. J. Flory, Statistical Mechanics of Chain Molecules, John Wiley & Sons, Inc. (1969).
19. M. B. Rhodes and R. S. Stein, J. Polym. Sci., (Physics), 1, 1534 (1969).

REFERENCES (Cont'd)

20. T. Hashimoto, T. Ijitsu, K. Yamaguchi, and H. Kawai, Polym. J., 10, 745 (1980).
21. P. J. Flory, Proc. Roy. Soc., London, A234, 73 (1956).
22. W. H. Chu and D. Y. Yoon, J. Polym. Sci., Polym. Symp., 61, 17 (1977).
23. W. W. Adams, Private Communications.
24. G. C. Berry, AFML-TR-71-2, Part VII, August (1977).
25. P. J. Flory, Angew. Chem., 87, 787 (1975).
26. P. J. Flory, Ber. Bunsenges, Phy. Chem., 81, 885 (1977).
27. A. K. Gupta, H. Benoit, and E. Marchal, Europ. Polym. J., 15, 285 (1979).
28. S. R. Allen, A. G. Filippov, R. J. Farris, and E. L. Thomas, J. Appl. Polym. Sci., 26, 291 (1981); E. C. Chenevey and E. W. Choe, AFWAL-TR-80-4142, October (1980).
29. W. W. Adams, L. V. Azaroff, and A. K. Kulshreshtha, Zeits. fur Kristal., 150, 321 (1979).
30. E. J. Roche, T. Takahashi, and E. L. Thomas: A. French and K. Gardner, Eds., Fiber Diffraction Methods, ACS Symp. Ser. #141, pp 303-314, Amer. Chem. Soc., Washington, D.C. (1980).